LHC ICP-Internal Note 00-199

1999-10-27

Author: Florian.Sonnemann@cern.ch

Review of quench simulations for the protection of LHC main dipole magnets

A. Danner, F. Sonnemann LHC/ICP

Keywords: superconductivity, LHC main dipole magnets, quench protection, quench simulation

Summary

The simulation program QUABER [1] allows studying the quench process of superconducting magnets for the LHC. The performance of the protection system of the LHC main dipole magnets was simulated under various parameter dependencies at different magnet excitation currents. This simulation study was motivated to complement measurement results in order to help preparing and understanding experiments of the quench propagation and magnet protection.

The influence of the quench propagation velocity and the time for a quench propagation between adjacent turns was studied. The different copper plating cycles of the quench heater strips were simulated. Experimental measurement results [2] were used to calibrate the input parameters. The performance of the protection system for various quench detection thresholds was investigated and different failure modes of the system were considered. The maximum voltages and values of the quench load are discussed.

The values given are obtained using conservatively chosen parameters. The quench back effect is modelled at high currents by quenching the entire inner layer at a certain time after the quench start. The temperature evaluation is based on adiabatic calculation.

The main results of the study can be summarised as follows:

- Realistic values for the quench propagation were used to determine adequate detection parameters, i.e., a quench propagation velocity of about 15-20 m/s at nominal current and a time for quenching adjacent turns of about 20-30 ms were set for nominal current. Heater delays of 30ms (high field heaters) and 50-60ms (low field heaters) were used. It was shown that the detection should not be exceed a threshold at 0.2V and a validation integration time of 5 to 10 ms.

- The high field heaters alone are sufficient to protect the magnet even when a conservative assumption for the quench starting in the inner layer is made (for nominal current, at lower current no quench of the inner layer is assumed). This study also demonstrated the importance of the quench propagating into the inner layer. When a quench in the inner layer is excluded, the quench load value reaches very high values independent from the heater strip configuration.

- The turn on voltage of the power diode that is installed in parallel to each magnet is reached at any current even if the heaters fail, i.e., they are unable to provoke a quench a low magnet currents. The diode alone is able to protect the magnet up to a current of about 2.3kA. Above that value, quench heaters are required.
- The quench heater study includes the systematic investigation of different heater delays, failing of one or several heater strips, and different copper plating cycles. The copper plating cycle was found to have little influence on the protection. The voltages inside the magnet can reach values up to 1 kV due to scattering heater delays or failing quench heater channels. The model that allows asymmetric quenching of the magnet was also used to reproduce an accidental quench of the first six block 15m long prototype dipole magnet that is being tested at CERN.

---

1. Introduction

The main dipole magnets of the LHC will be protected by quench heaters that are fired after a quench detection of and parallel diodes. The firing of quench heaters ensures a more uniform distribution of the stored magnetic energy and the current bypasses the magnet and flows through the protection diode after the resistive voltage exceeds the turn on voltage of the diode.

The performance of the protection system for the MB dipole magnet relies on a number of different parameters [3]. Among these are the threshold detection voltage, used to trigger the protection system, and the heater delays that determine when quench heaters become effective after having been fired. The parameter studies described below are carried out to better understand experimental results and to improve the definition of the QUABER magnet models for future work. A comprehensive study was conducted to provide detailed cause-and-effect relationships between different magnet parameters. The calibrated simulation data on hot spot temperature, quench load, resistance developed, etc. was compared resulting from various scenarios.

The different simulation can be grouped as follows:

- *Model study*: Determine to what extent uncertainties in the following parameters affect the results from, and usability of, the QUABER model, as well as how measurement results from a real magnet may be affected because of these parameters:
  turn-to-turn quench propagation delay
  quench propagation velocity
  RRR of copper matrix of the conductor
  copper plated and heated part lengths
  location of quench origin

- *Magnet current effects*: Qualif heater delays at various detection voltages and current levels, both for single magnets and series magnets. The resistance development, quench load and hot spot temperature is recorded. The main goal is to help determining acceptable threshold detection voltages.

- *Failures:* Determine the consequences of component failures on a magnet for various currents and conditions. This includes the failure of heaters placed in the high field region, those placed in the low field region and the failure of the protection diode (current cannot bypass by flowing through the diode).

- *Heater study:* A comprehensive study of the interactions between the various heater delays, for both single and series magnets, is carried out to help determining the required detection level.

- *Aperture quenching asymmetries:* The effects of timing differences (scattering) between apertures of heater firings and of the complete heater firing failure of one aperture are examined.

2. MB dipole magnet simulation studies

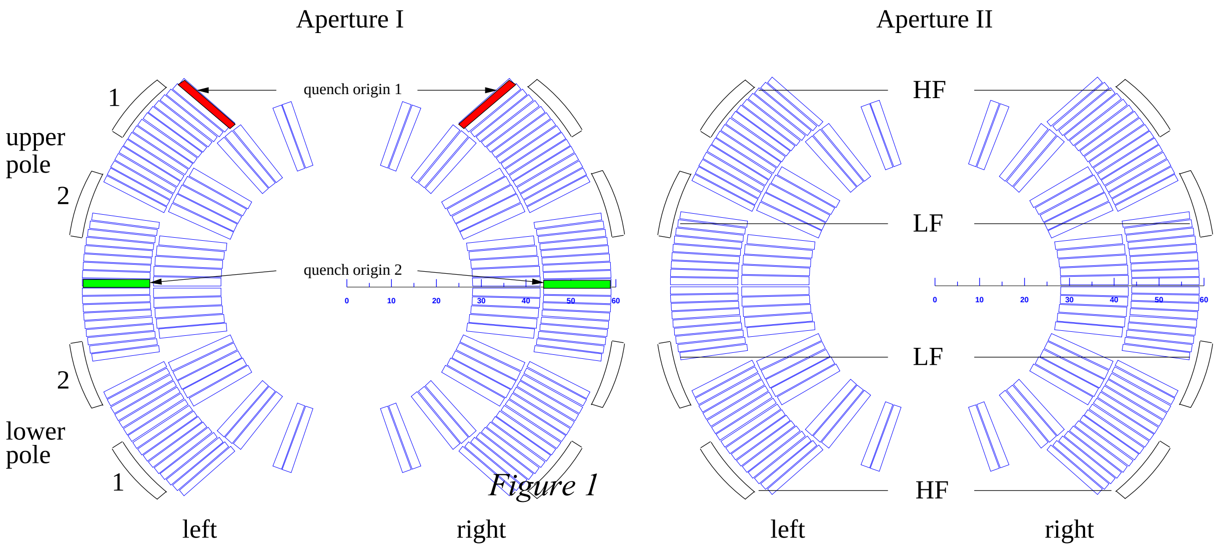

Figure 1

As shown in the above cross section (Figure 1), the MB dipole magnet consists of two apertures, each possessing eight heaters stips. The HF “high field” heaters (strips 1) are located in the high field region of the magnet, whereas the LF “low field” heaters (strips 2) are in a low field region. In the majority of these studies, at time t = 0, the quench will be assumed to originate in the high field region of the outer layer (*quench origin 1*) [2]. QUABER simulates the propagation of the quench throughout the other turns of the magnet, taking into account the firings of the heaters. In these studies, the inner layers are quenched artificially at a time which is adjusted according to experimental results, allowing the effects of quench-back and time of inner layer quench to be emulated more accurately.

The results obtained from QUABER are the values of the hot spot temperature, quench load, resistance developed, current decay, maximum voltage and the time required to reach the maximum voltage. The temperatures in these simulations are calculated adiabatically, i.e. cooling effects are neglected. Figure 2 shows conversion charts between quench load, and resistivity versus temperature for the cables used in the magnet studies. Note that the magneto resistance is only significant at temperatures below 80 K, above which it is a function only of RRR and temperature.

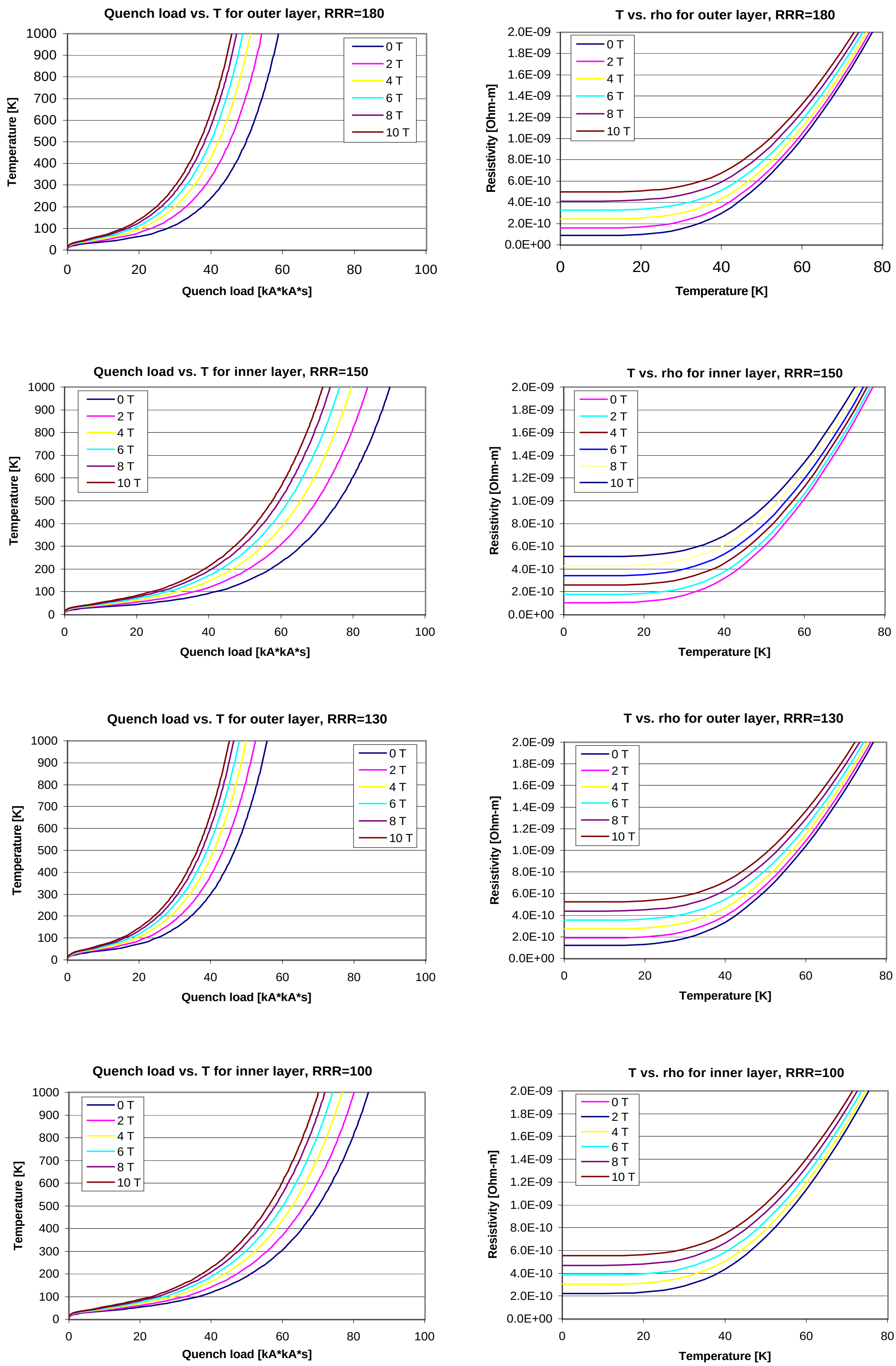
Quench load vs. T for outer layer, RRR=180
Temperature [K]
Quench load [kA*kA*s]
0 T
2 T
4 T
6 T
8 T
10 T
T vs. rho for outer layer, RRR=180
Resistivity [Ohm-m]
Temperature [K]
0 T
2 T
4 T
6 T
8 T
10 T
Quench load vs. T for inner layer, RRR=150
Temperature [K]
Quench load [kA*kA*s]
0 T
2 T
4 T
6 T
8 T
10 T
T vs. rho for inner layer, RRR=150
Resistivity [Ohm-m]
Temperature [K]
0 T
2 T
4 T
6 T
8 T
10 T
Quench load vs. T for outer layer, RRR=130
Temperature [K]
Quench load [kA*kA*s]
0 T
2 T
4 T
6 T
8 T
10 T
T vs. rho for outer layer, RRR=130
Resistivity [Ohm-m]
Temperature [K]
0 T
2 T
4 T
6 T
8 T
10 T
Quench load vs. T for inner layer, RRR=100
Temperature [K]
Quench load [kA*kA*s]
0 T
2 T
4 T
6 T
8 T
10 T
T vs. rho for inner layer, RRR=100
Resistivity [Ohm-m]
Temperature [K]
0 T
2 T
4 T
6 T
8 T
10 T

Figure 2

The electrical layout of the MB dipole magnet is shown in Figure 3. For our studies, the quench begins at t = 0. After a given time (see Table 1), the switch opens across the extraction resistor and the power s upply is switched off to emulate conditions in the actual

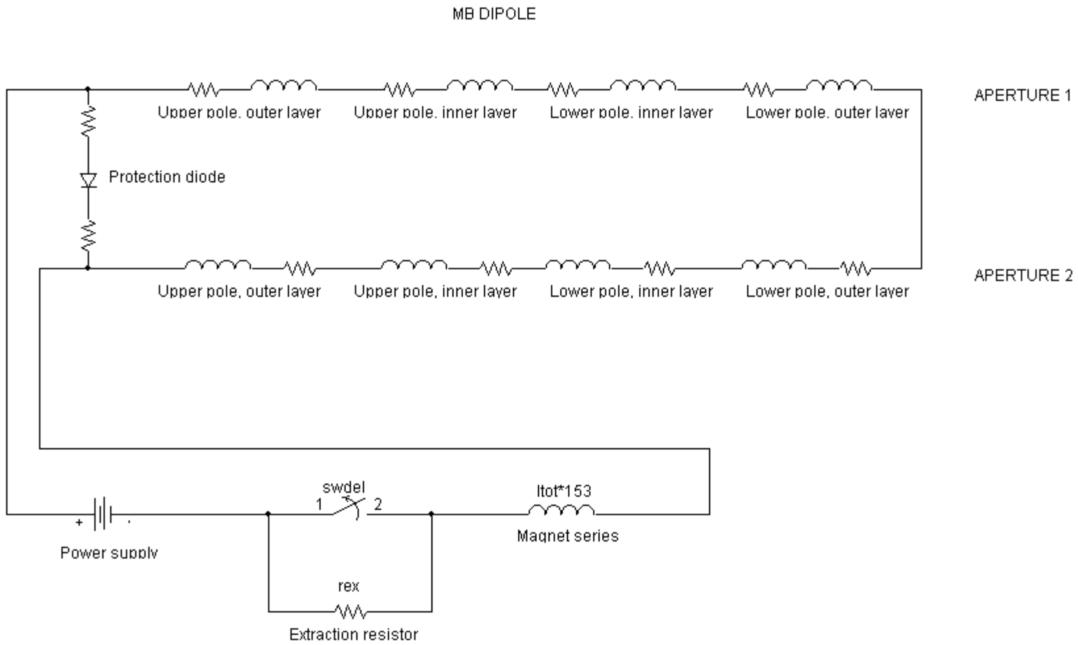

Figure 3

Variable	Description	Typical value
b_m	peak magnetic field	8.61335 T
cssdt	time at which voltage source is switched to 0 V	24.1 ms
ht_delay_high r	aperture 2 high field heater delay	54.1 ms
ht_delay_high_l	aperture 1 high field heater delay	54.1 ms
ht_delay_in1	aperture 1 time of inner layer quench	125.9 ms
ht_delay_in2	aperture 2 time of inner layer quench	125.9 ms
ht_delay_low_l	aperture 1 low field heater delay	75.9 ms
ht_delay_low_r	aperture 2 low field heater delay	75.9 ms
i0	nominal current	11796 A
len_cu	copper plated length of the heater strip cycle	40.0 cm
len_heat	heated length of the heater strip cycle	12.0 cm
ltot	total inductance for one magnet in the series	0.1074 H
quench_velocity	quench velocity at initial current	2000 cm/s
rex	external extraction resistance (single magnet)	20 mΩ
rex	external extraction resistance (magnet series)	150 mΩ
swdel	time after start of quench to switch in extraction resistor	24.1 ms
ttx	quench propagation between adjacent turns	30 ms

Table 1: Parameters studied

magnet. When the resistive voltage across the magnet reaches the turn-on voltage of protection diode (8.3 V is used at 1. 8 K), current begins bypassing the magnet through the diode. Different parameters are studied using this model. See Table 1 for a short description of each. All times are measured from start of quench.

Constant parameters are set to the values in Table 1 unless otherwise noted. Cable parameters for the MB dipole magnet used in the simulation studies are shown below. The majority of simulations were conducted with RRR=180 and RRR=150, respectively (although as will soon be apparent, the inner layer RRR makes little difference for the quench performance).

Parameter	Outer layer	Inner layer
RRR	180, 130	200, 150, 100
Ratio Cu/NbTi	1.9	1.6
Copper area [cm*cm]	0.126083	0.153495
NbTi area [cm*cm]	0.066359	0.095934
Total cable width [cm]	0.173855	0.214005
Metal width [cm]	0.127445	0.168533
Total cable height [cm]	1.54	1.51
Total metal height [cm]	1.51	1.48

Table 2: Cable parameters

The QUABER setup for a single magnet is shown below. The quench begins at orig.ou1, and progresses through the other turns of the first aperture. Heater "heat.xxx" elements are fired after detection and their effects are felt by nearby turns not covered by heaters (the passive "pass.xxx" elements) according to the turn-to-turn propogation time *ttx*. The ghost element is included to satisfy QUABER's connection requirements [1] and has no effect on the electrical behaviour of the circuit. The inner layers of the magnet are quenched artificially using QUABER "heat.xxx" elements, whose quench times can be precisely controlled to model behaviour of actual magnets.

MB DIPOLE (SINGLE MAGNET) QUABER SETUP

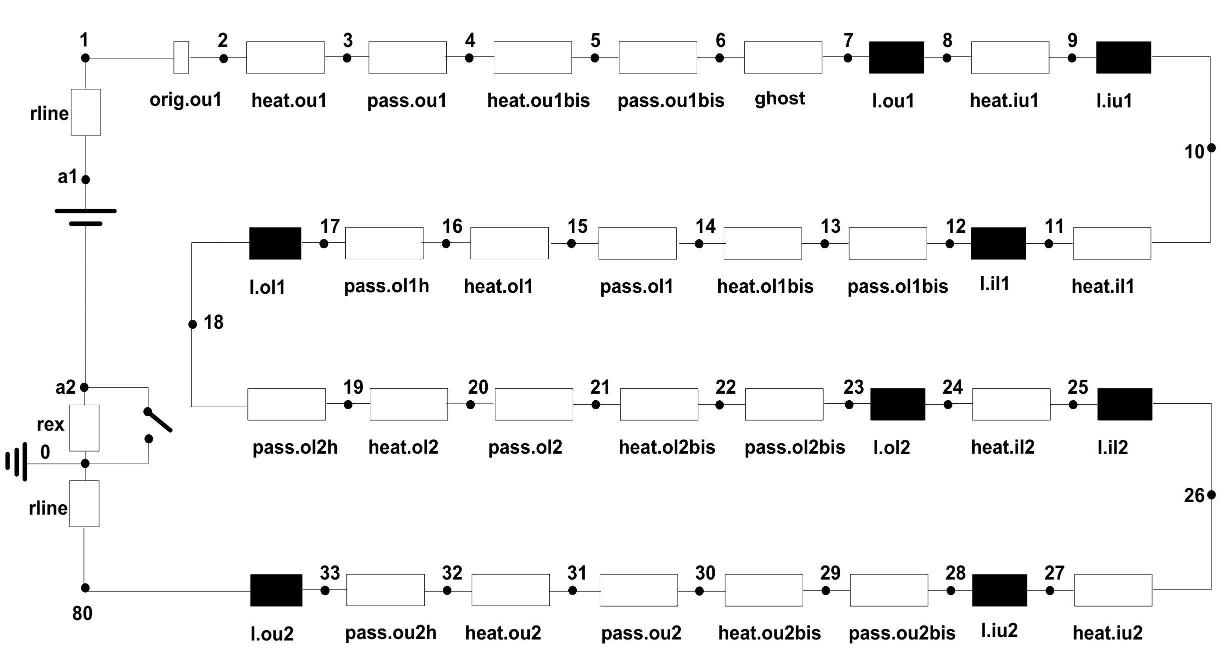

Figure 4

2.1. Model study

2.1.1. Accuracy

Many of the graphs presented in these studies present the quench load versus a certain parameter. The unit to be used for the quench load is the MIIT, or kA*kA*s, calculated by as follows:

$$\text{MIIT} = \int_0^\infty I^2 dt \text{ in units of kA*kA*s} \quad (1)$$

The starting time *0* stands for the start of the propagating quench. The accuracy of QUABER is limited by the time step of the simulations. At 0.2 V detection, nominal current, there is a 0.4 MIITS increase in quench load when the time step is increased from 5 ns to 30 ns, and a further increase of 0.3 MIITS when 50 ns is reached. The accuracy of the model is therefore limited by approximately 0.7 MIITS (All simulations were carried out within this range.) However, any errors such as this induced by time step differences were global, i.e. trends in results did not change with the time step, and larger time steps gave more conservative data, as in the above case. All data for a given study was collected from QUABER using the same simulation time step.

Quench detection in an actual magnet will occur by measuring the voltage between the two apertures through a bridge circuit, and triggering magnet protection when a threshold, 0.2 V for example, is detected. In the QUABER models the total magnet voltage is measured to give the detection voltage. In the actual bridge circuit, there is a resistive voltage divider that reduces the detection voltage by a factor of two. Thus, to convert the detection voltages presented here into the actual voltages that must be detected by the circuit, one must divide by two. For example, a 0.2 V detection level actually corresponds to a 0.1 V output from the bridge that feeds into the detection circuitry.

2.1.2. Turn-to-turn quench propogation time (*ttx*)

The results of the simulations presented in Figure 5 cover the entire range of pessimistic and optimistic values for the propagation time between adjacent turns of the MB dipole magnet. The value normally used is *ttx* = 30 ms between adjacent turns in the cable. If this value is changed by 25 ms, the value of quench load changes up to 1 MIITS. These simulations were carried out holding the switch delay and all heater firing times constant. In reality, a change in the turn-to-turn delay would also cause a change in detection time, not considered here.

2.1.3. Quench propogation velocity (*quench_velocity)*

This parameter is the velocity of the quench down the length of the magnet, i.e. perpendicular to the cross section of Figure 1. Measured values of quench velocities at nominal current are about 1500 cm/s to 2000 cm/s [4]. This type of uncertainty has little effect on the model (see Figure 6). As above, these simulations were carried out holding the switch delay and heater firing times constant.

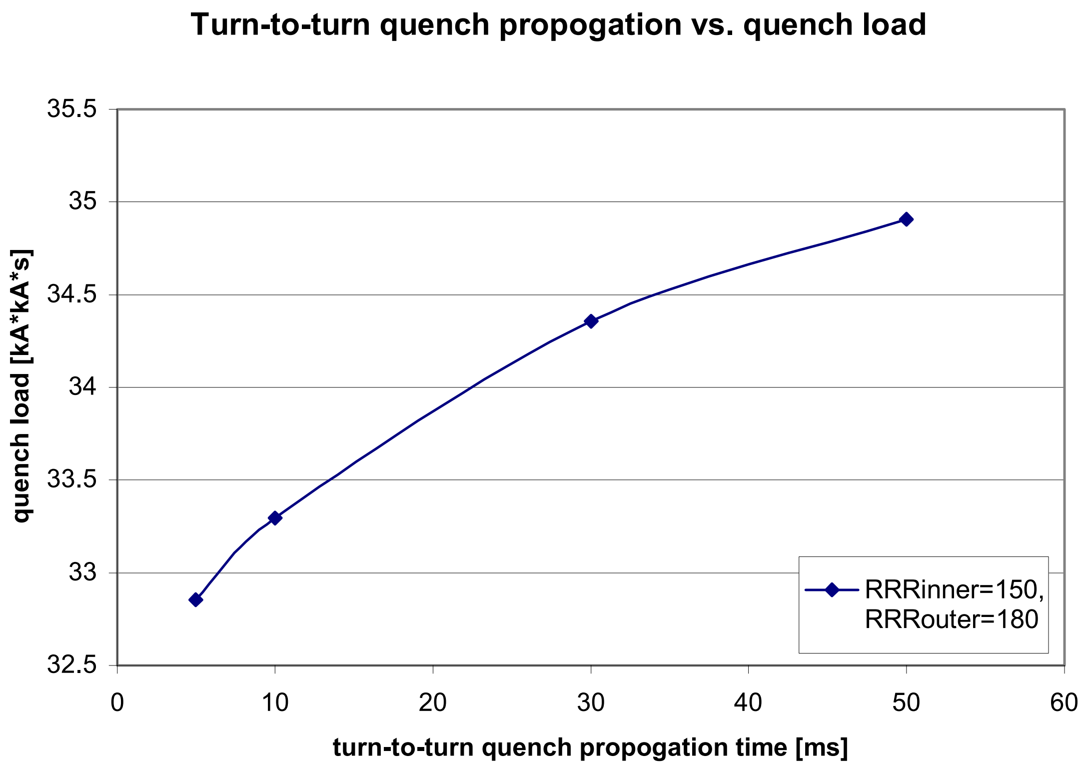

Figure 5

2.1.4. RRR

In both studies above, simulations were carried out with two different sets of RRR values. Although not presented in the graphs, there is a constant relationship between the two. If the

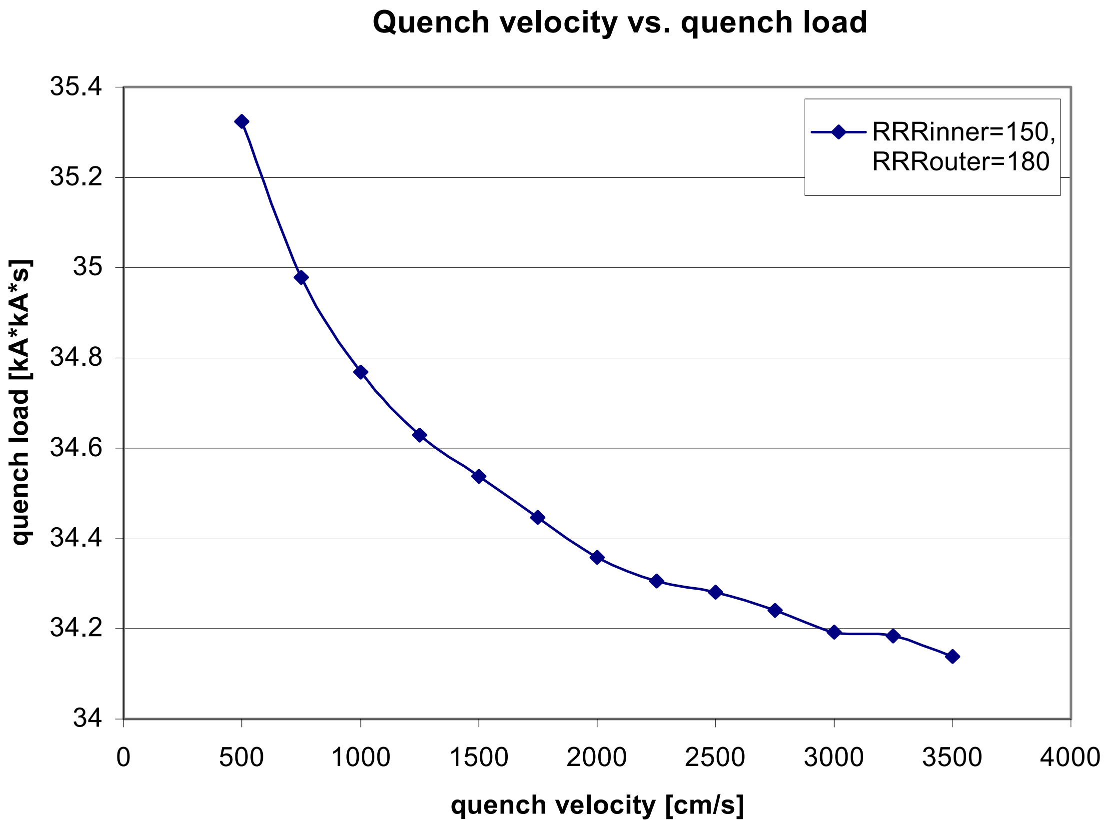

Figure 6

outer RRR value is lowered from 180 to 130, the corresponding quench load decreases by 1.2 MIITS in both studies in a linear fashion. However, quench loads are not easily compared since the change in RRR also affects the hot spot temperature in the opposite way. In these cases, this decrease of 1.2 MIITS corresponds to a decrease in hot spot temperature of approximately 7 K. Usually, one might expect a lower RRR to increase the hot spot temperature. However, at low temperatures, a lower RRR means an increased resistivity (see Figure 2). This causes faster resistance development and current decay, resulting in these lower temperatures. A value of RRR = 180 is used exclusively in further studies. As above, these simulations were carried out holding the switch delay and heater firing times constant.

Since the inner layer is quenched late, and all turns are quenched at the same time in this model, the RRR of the inner layer has only a small effect on quench load. With both 0.1 V and 0.2 V detection, the rise in quench load caused by an increase in the inner layer RRR from 150 to 200 (with outer layer RRR held constant at 180) was only 0.09 MIITS in both cases. This difference is negligible, as it is beyond the general time step accuracy of the model.

2.1.5. Copper and heaters lengths (*len_cu* and *len_heat*)

The interaction between lengths of copper plated and heated parts of the heater cycles was studied holding other values constant. As expected, the lowest quench load occurred with the greatest heated length. Using the greatest length, of course, is not feasible because the energy needed to fire such a heater is too large, but this shows that small changes in the heater design should not have large influences on resulting quench loads.

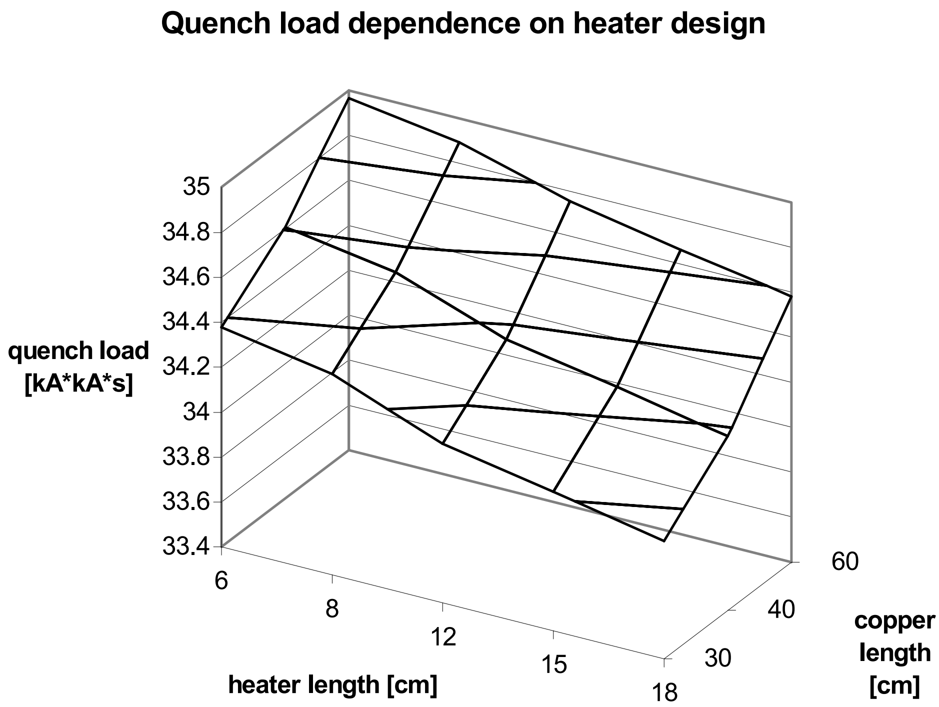

Figure 7

2.1.6. Quench origin

The most likely place for a quench is in the high-field region of a magnet, since the presence of a stronger magnetic field lowers the critical temperature for superconductivity. This study compares detection times at various voltages for a quench starting (see Figure 1) in a high field region (quench origin 1), and a low field region (quench origin 2). For detection at 0.1V, 6.5 additional milliseconds were required to detect the quench at quench origin 2 with respect to quench origin 1. Detecting at a threshold of 0.2 V, 11.3 additional milliseconds were needed for detection. Table 3 summarises these results for outer layer RRR = 180 and 150 (in parentheses).

Detection voltage [V]	Detection time, quench origin 1 RRR=180 (RRR=150) [ms]	Detection time, quench origin 2 RRR=180 (RRR=150) [ms]
0.1	19.1 (12.4)	25.6 (19.2)
0.2	26.1 (18.7)	37.3 (31.0)
0.3	31.1 (24.6)	46.0 (38.9)
0.5	41.4 (34.9)	58.4 (49.7)

Table 3: Quench origin effects

The expected differences will have two main causes:

- Resistance development takes place more slowly in the low field region, resulting in later detection times
- The quench velocity is lower, and although not taken into account above, will serve only to enhance these differences in detection times

2.2. Magnet current effects

In order to study how different current levels affect the protection, the times required to reach different detection voltage levels must be found. To determine the appropriate switch delay (*swdel* in Table 1) to use in the computer model, simulations were run with no heater firings, and the time was noted at which the desired voltage level (whole-magnet voltage) was reached. The table below summarises the results. A 5 ms validation period was added to the detection time to obtain the final values for the switch delays. This shows, in essence, the time it takes to detect a quench at various current levels and for different detection times.

current [kA]	t(.1V) [ms]	t(.2V) [ms]	t(.3V) [ms]	t(.5V) [ms]
0.800	824.5	1442.4	2060.2	3268.8
1.500	332.1	497.8	656.5	968.0
3.000	128.3	179.2	233.2	304.3
4.500	77.6	109.9	124.2	167.1
6.000	57.6	73.2	80.9	111.2
9.000	26.7	35.9	47.3	59.4
11.796	19.1	26.1	31.1	41.4

Table 4: Current effects

Heater delays were then calculated by adding certain offsets to the switch delays. The high and low heater delays used for these tests were calculated using the following formulae [2], producing expected values:

$$ht\_delay\_high = 270e^{-0.185I[kA]}[ms] \quad (2)$$

$$ht\_delay\_low = 270e^{-0.14I[kA]}[ms] \quad (3)$$

The quench velocity, turn-to-turn propagation time and peak magnetic field were scaled appropriately to each current level in all tests.

To determine which detection threshold will be appropriate, quench loads and hot spot temperatures obtained through quenches at various currents and detection threshold levels were compared. (See Figure 8.) +
Between the levels of 0.1 V and 0.5 V, there is a significant 99.71 K difference in hot spot temperature and 3.072 MIITS at nominal current. With an adiabatically-calculated hot spot temperature of 477.09 K at 0.5 V detection, 0.5 V would be an unacceptable detection level. Under adiabatic conditions, a 0.2 V detection level appears to produce a rather high temperature as well (406.5 K), but suggests that this would be an acceptable detection threshold for the magnet protection system under appropriate cooling conditions. Note that this corresponds to an output to the detection circuit of 0.1 V because of a voltage divider in the detection bridge.

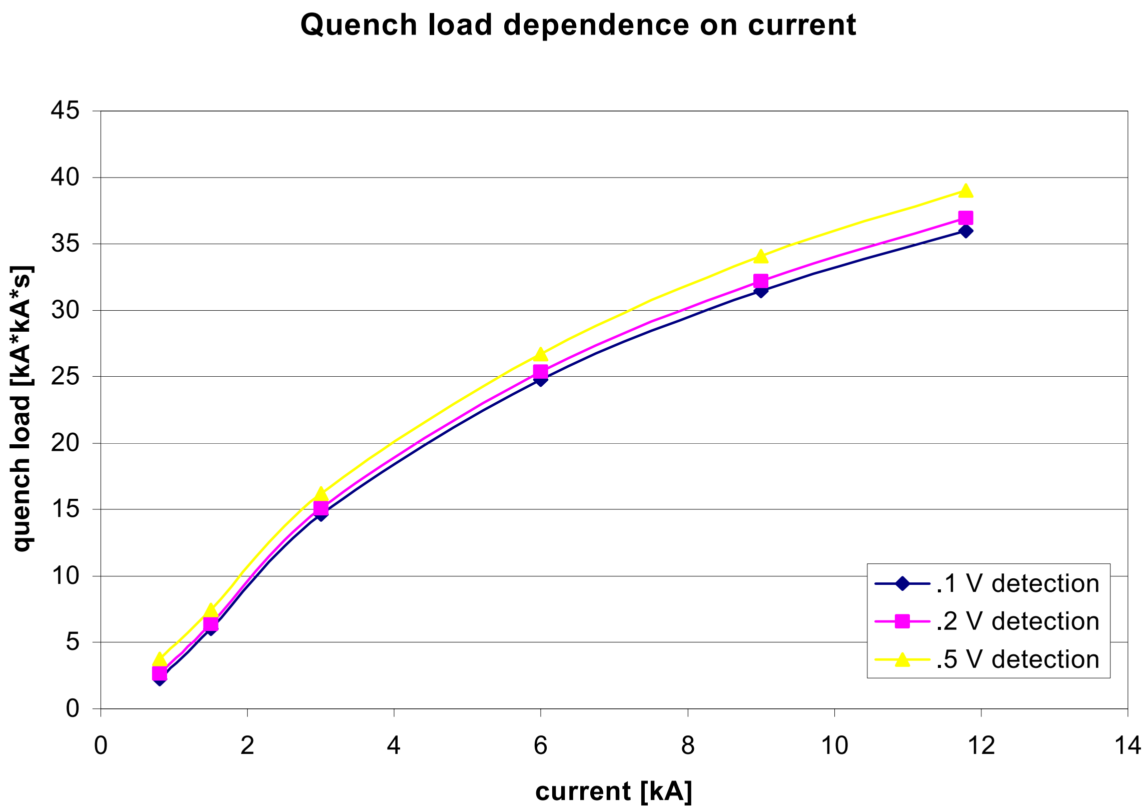

Figure 8

The detection level plays an unimportant role in the resistance development, which is governed almost entirely by the current, as can be seen in the following equation used for its calculation:

$$resdev = \frac{v\_magnet - L\frac{di}{dt}}{i} \tag{4}$$

where *resdev* is the resistance development, *v_magnet* is the voltage across the magnet, *L* is the magnet's inductance, and *i* is the current flowing through the magnet (see Figure 9). A second order polynomial curve fit was applied to the simulation results. The results show that the QUABER model is operating properly, as the energy dissipated into the magnet after a quench goes quadratically with the current.

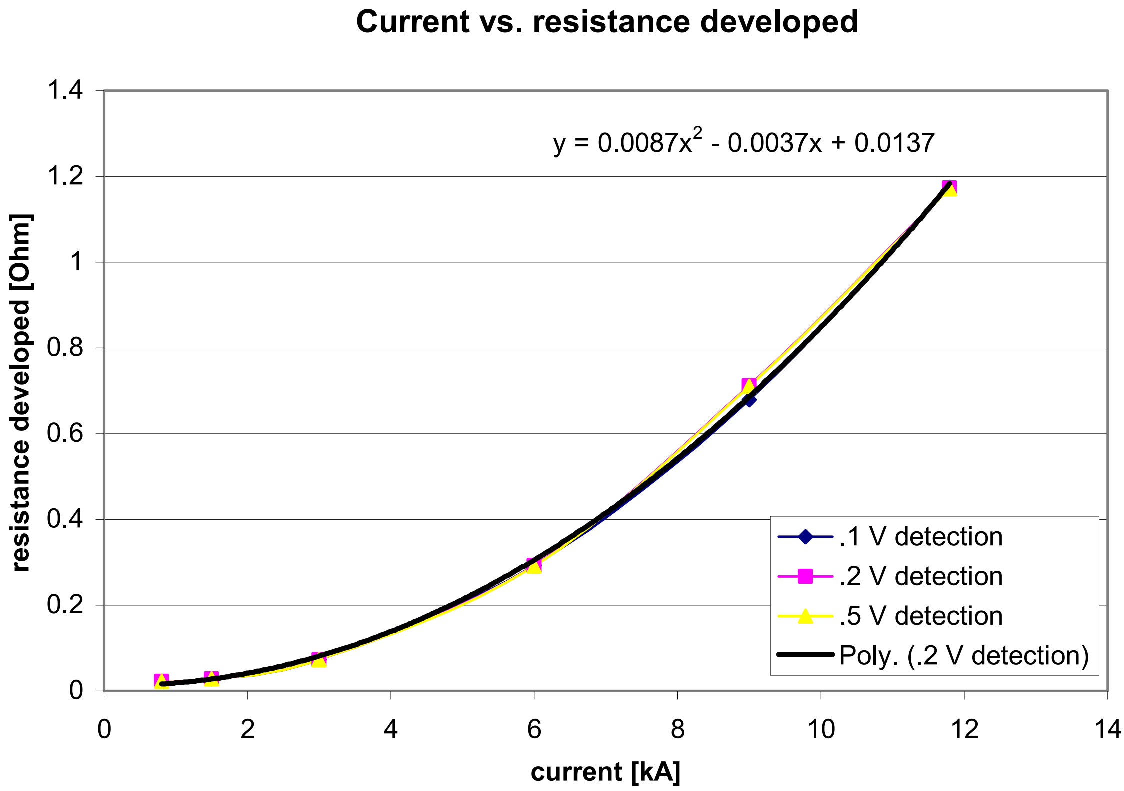

Figure 9

2.3. Failure modes

2.3.1. Heater failures

A quench at full current (11.796 kA) that is detected at a threshold of 0.2V detection and a validation period of 5ms would cause a quench load of 62.5 MIITS and a corresponding adiabatically-calculated hot spot temperature of 2061 K, if heaters failed (considering no quench in aperture 2 and inner layers, natural quench starts in aperture 1). A magnet under these conditions would be seriously damaged. However, this situation is unrealistic. In reality, the quench would spread throughout the entire magnet and quench-back would occur.

Quench-back is an effect caused when the rest of the magnet, i.e., the parts not near the quench origin, quench due to eddy currents. The eddy currents are generated due to a strong dB/dt during a current decay after a quench. The eddy currents go via contact resistances between strands of the superconducting cable, causing heat to be generated. If the temperature exceed the critical temperature, the quench-back starts. A recent quench of a 15-m long dipole magnet (MBP2N1v2) produced, when heaters were unable to fire, a quench load of 43 MIITS [5]. To duplicate this effect in a simulation, three regions of a magnet were artificially quenched at a certain time in a computer model. The following times resulted in obtaining an identical quench load of 43 MIITS:

Magnet region	Simulated quench time
High field region, outer layer	145 ms
Low field region, outer layer	175 ms
Inner layer	240 ms

Table 5: Matching simulations to test data

This gives some indication as to the importance of including quench-back effects into a simulation model, as is done in the heater study. It is not accounted for in this failure study because quench-back at low currents is unlikely.

Simulations were carried out to determine the point at which the magnet is endangered, not assuming quench-back. At lower currents (under 3 kA), the quench load remains under 38.8 MIITS regardless of detection threshold. If a quench were to occur during injection, even with a heater failure, the magnet would be safe. Notable here is the fact that the protection diode still turns on, even if heaters fail at 0.8 kA. The quench detection, as can be seen in Figure 10, plays only a small role in this study. The differences at lower currents are caused by longer differences between detection times, which converge at high currents.

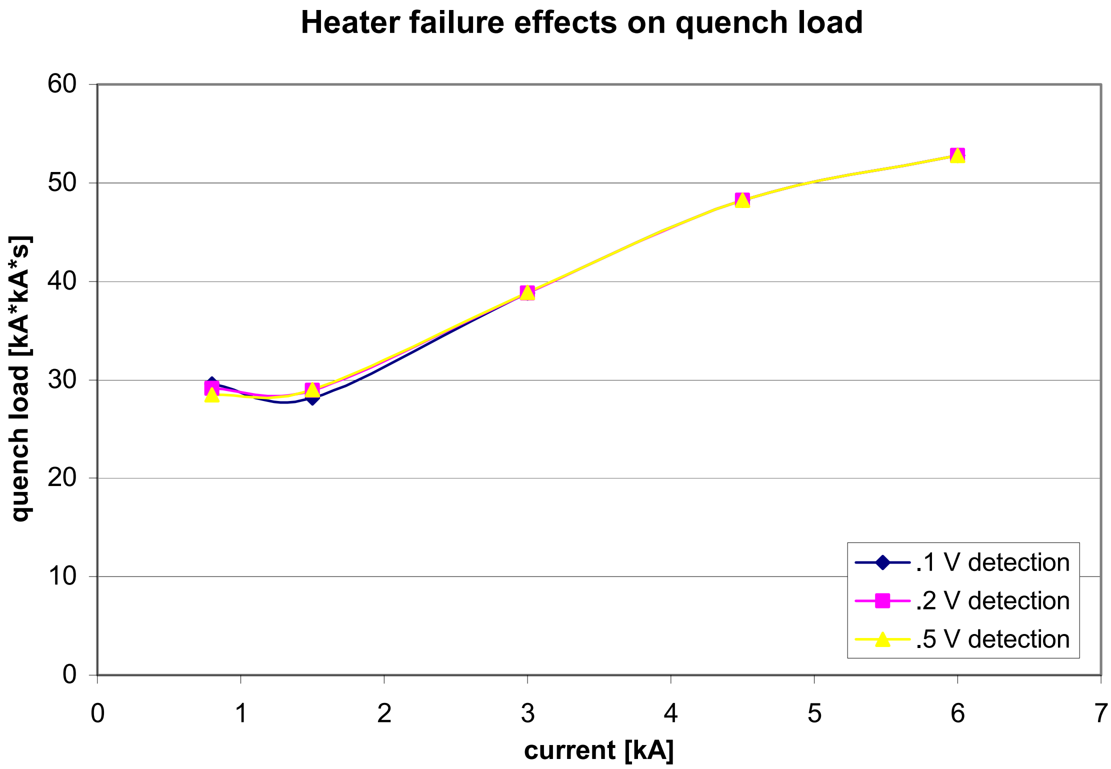

Figure 10

If the nominal current were under 2-3 kA (possibly higher with quench-back effects), heater strips would be unnecessary, since the magnet is inherently safe at those currents.

Heater position plays an important role in quench protection. Presented below are situations at nominal current, 0.2 V detection with 5 ms validation period (quench-back effects included as indicated). The offsets given are time from detection at which heaters become effective. If low field heaters fail or are not fired, the high field heaters alone are able to protect the magnet adequately in this model. However, low field heaters alone cannot protect the magnet with the assumed parameters if high field heaters fail. New experimental results showed that LF heaters alone might be able to be sufficient due to change heater parameters that reduces the heater delays. The inner layer quench has less effect.

High field heater offset [ms]	Low field heater offset [ms]	Inner layer quench time [ms]	Quench load [kA*kA*s]
30.4	51.8	101.8	35.67
30.4	51.8	no quench	36.63
30.4	no firing	101.8	36.87
30.4	no firing	no quench	40.61
No firing	51.8	101.8	43.93
No firing	51.8	no quench	46.95

Table 6: Efficacy of low and high field heaters

2.3.2. Protection diode failures

Although extremely unlikely, a protection diode failure in which current is blocked, i.e. the diode failure creates an open circuit instead of a short, would seriously damage a magnet at high current. Studies were not carried out for currents above 3 kA, since a quench at this current causes quench loads of 54.5 MIITS at 0.1 V detection and 65.1 MIITS at 0.5 V detection, and corresponding adiabatic hot spot temperatures of 960.5 K and 1080.6 K, respectively, which would be too problematic for the magnet. If a quench were detected immediately upon injection, however, regardless of the detection threshold used, the magnet would still be protected even with this type of failure (see Figure 11).

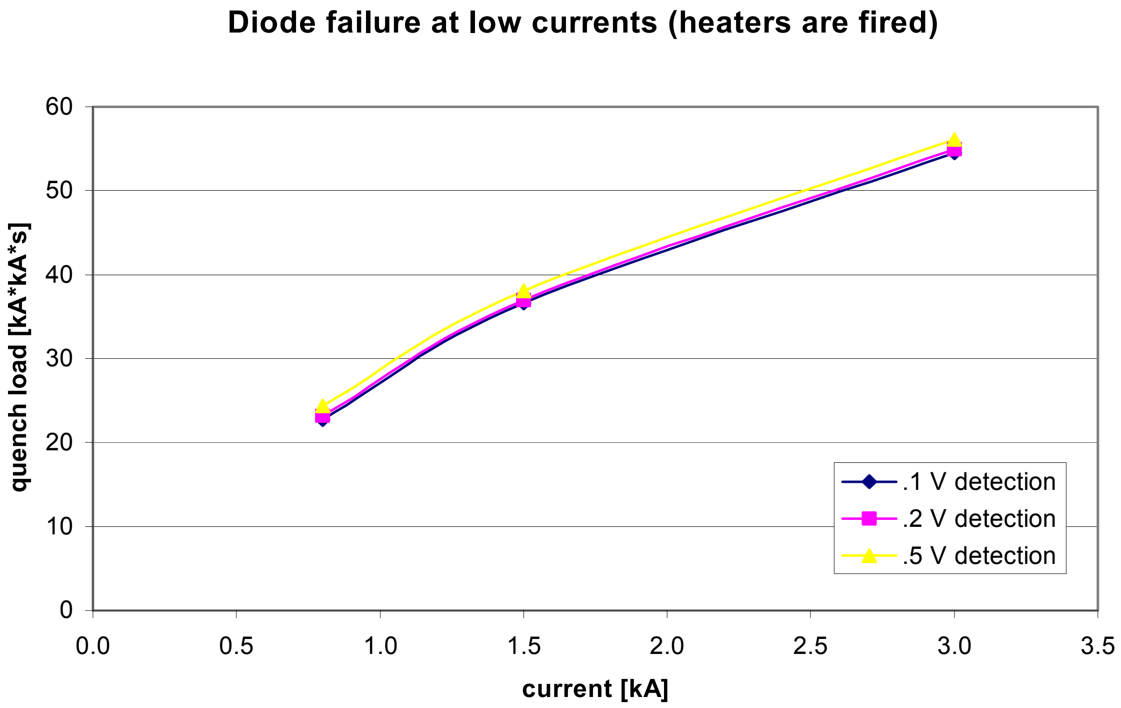

Figure 11

3. Heater study

To show the effect of heaters in the MB dipole, voltages from the simulation of a quench of a single magnet in which all heaters were fired at the same time (250 ms) are shown below. The quench was also forced to start in the inner layer at the same time to simulate the quench back effect. The other parameter settings are the extraction resistor *rex* = 27 mΩ, turn-to-turn delay *ttx* = 30.5 ms, and the initial current of 11.0 kA in this case. This test was motivated by the massive quench-back that occurred in test MBP2N1v2 when heaters were unable to be fired.

In Figure 12, at 50 ms, as a result of the detection of a quench, the voltage source is switched off and the extraction resistor immediately becomes the most resistive part of the circuit. For that reason all magnet voltages drop. Because the quench originates in aperture 1, upper pole, outer layer, the resistance from that element (orig.ou1, in this case) grows rapidly and causes a voltage rise. Without quench back, this voltage would continue to rise to just above 1500 V. In this case, however, the simulated quench back causes a sharp increase in resistance in the other parts of the magnet, causing the inductive voltage of the quench origin signal to dominate temporary. As can be seen, the inner layer voltages rise while the others fall. This is because the inner layers are all quenched at the same time, so when the inner layers quench their instantaneous resistance development is much larger in the simulation than those of the outer layers.

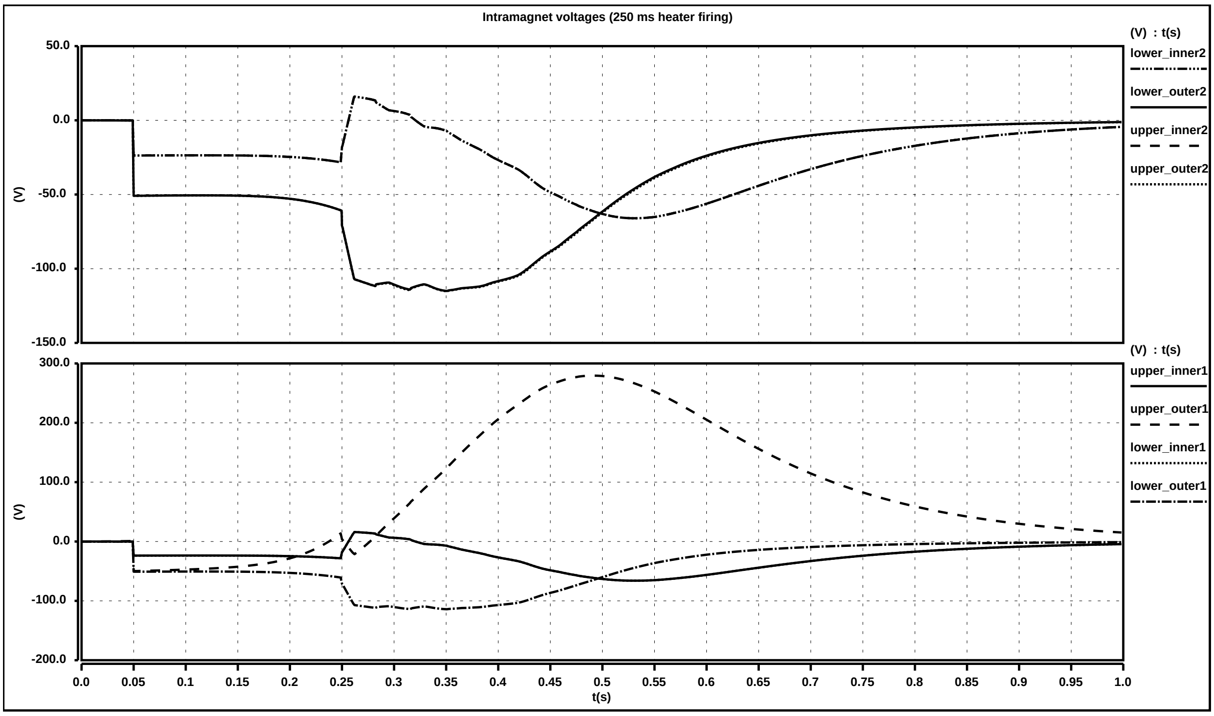

Figure 12

At 263 ms, the resistance voltage dominates again in the quench origin signal. This causes the voltage turn-around after which the quench propagation continues naturally.

The firing of the heaters causes an ultimate lowering in internal magnet voltages. This, in turn, affects the current decay and the quench load in a positive way. One aim of the heater simulations that follow (see Section 3.1) is to determine to what extent heater delays will be acceptable for the protection system to still function.

3.1. Comparison single magnet/magnet in series

The family size for the main dipole magnets is 154 magnets. These simulations compare induced quench load for a variety of detection voltages and delays. They were carried out using a 1500 cm/s quench velocity. Also, the switch delays/heater delays were held constant, not the detection voltages, so those indicated in Table 5 represent only approximate detection voltages. The average difference in quench load among the eight tests was 0.68 MIITS, and, as in Figure 11, this is similar for all tests. These tests represent the extreme values used in the main heater study, performed only on magnets in series. The results for a single magnet can be estimated by subtracting 0.68 MIITS from the quench load of an equivalent series magnet. The reason for this difference is that the fast current decay in a single magnet starts immediately when the heaters become effective, whereas in a series of magnets the turn on voltage of the diode has to be reached before the current starts to decay fast. Fast current decay means a time decay constant τ of 200 - 300 ms, whereas the decay time constant for the whole series of 154 magnets is about 100 s.

Indicator	Detection [V]	Validation time [ms]	Switch delay [ms]	High field heater delay [ms]	Inner layer quench time [ms]
1	0.1	5	24.1	54.1	134.1
2	0.1	10	29.1	59.1	139.1
3	0.2	5	31.1	61.1	141.1
4	0.1	5	24.1	59.1	189.1
5	0.1	10	29.1	64.1	194.1
6	0.2	5	31.1	66.1	196.1
7	0.5	5	46.4	76.4	156.4
8	0.5	5	46.4	81.4	211.4

Table 7: Description of single/series magnet tests

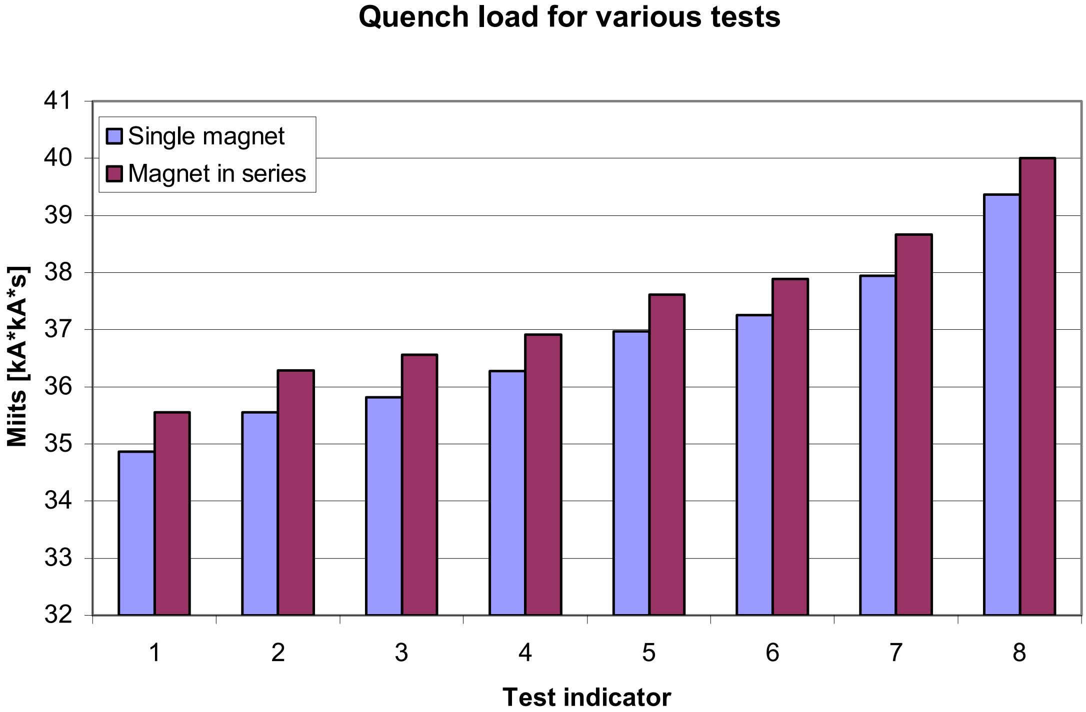

Figure 13

3.2. Series magnet heater studies

3.2.1. All heater delays varied proportionally

These studies were carried out using a quench velocity of 2000 cm/s and 0.1 V detection with a 5 ms validation period. With the switch delay held constant, the HF heater delay, i.e., time from start of quench when the high field heater becomes effective (including detection) was examined first. It was varied between 40 ms and 110 ms while the LF heater delays and inner layer quench times were adjusted linearly, with the LF heaters always firing 15 ms after the HF heaters, and the inner layers quenching 100 ms later. This study was performed for two RRR sets (see Figure 12), although they should not be compared with each other, as the quench load refers to a different temperature for the two RRR sets (see Figure 2). This shows, in effect, the overall efficacy of the heaters. The quench load is approximately 20 – 30 MIITS lower than in the case where the heaters fail.

The HF heaters were then held constant at 53.5 ms while LF heaters and inner layer quench time were adjusted linearly as above. The LF heaters are not as effective as the HF heaters because they cover fewer magnet turns and exist in a low-field region (see Figure 15).

Finally, the HF and LF heater delays were held constant at 53.5 and 68.5 ms, respectively, while the inner layer quench was studied. Although not shown in Figure 14, as the inner layer quench time approaches infinity, the quench load approaches 35.4 MIITS. Compared to the effect of the heaters, the quench of the inner layer is negligible.

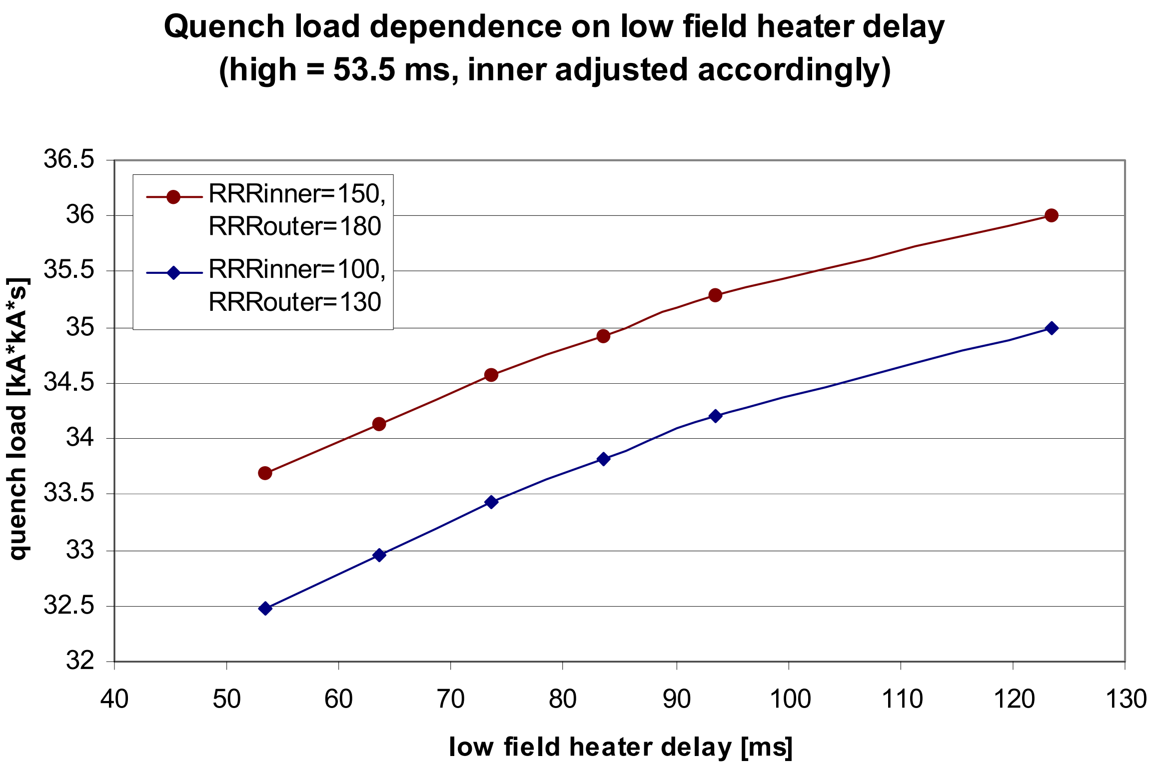

Figure 14

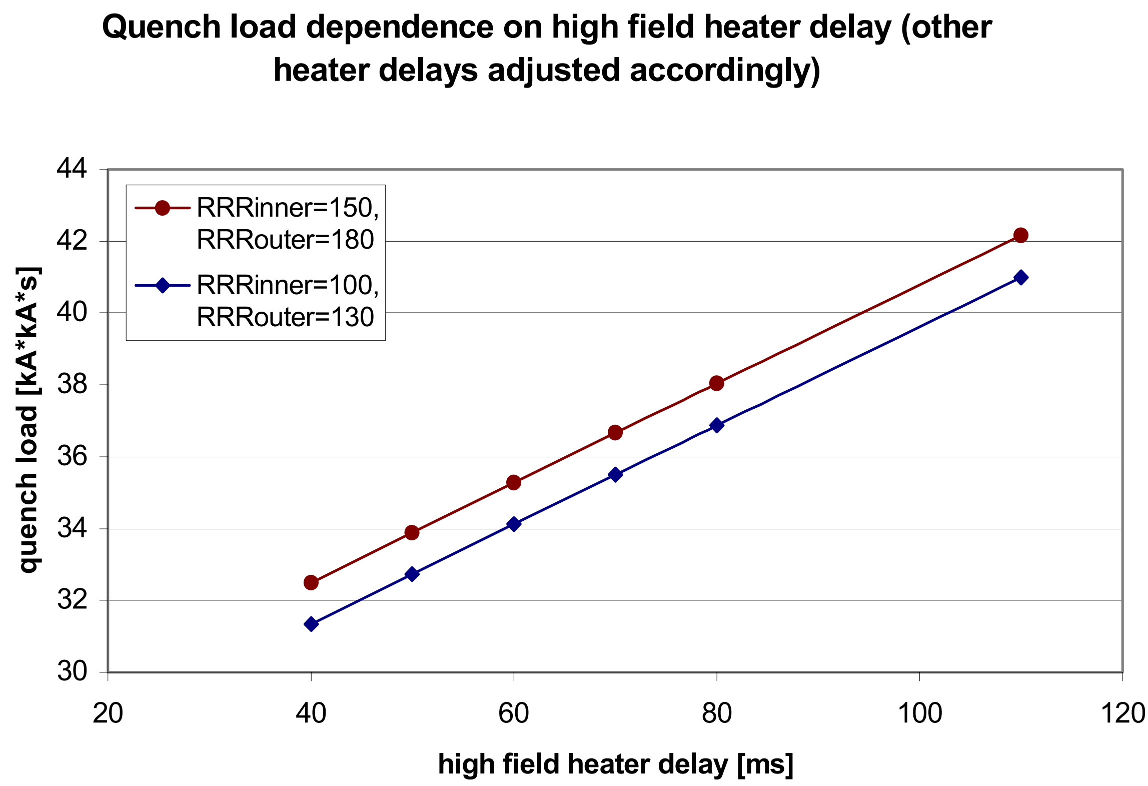

Figure 15

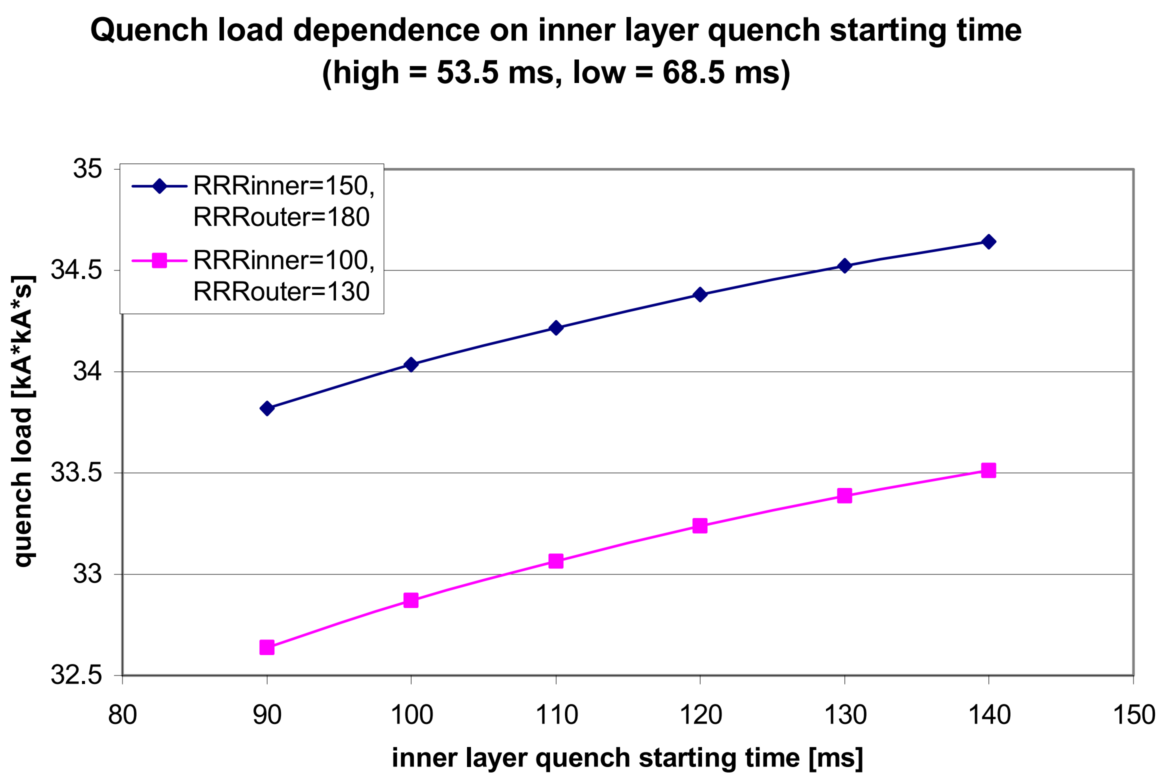

Figure 16

3.2.2. All heater delays changed independently

As can be seen in Figure 15, the inner layer quench has the least effect on quench load, and the firing of the high heater delay. A 0.2 V detection threshold was chosen for the majority of the studies because it has the greatest possibility of being implemented. Additionally, some tests were conducted at 0.1 V, as can be seen in Section 3.1, and at 0.5 V (see Appendix B). These studies were carried out with a quench velocity of 1500 cm/s. Results presented below use the offset, that is, time after detection and validation at which heaters become effective.

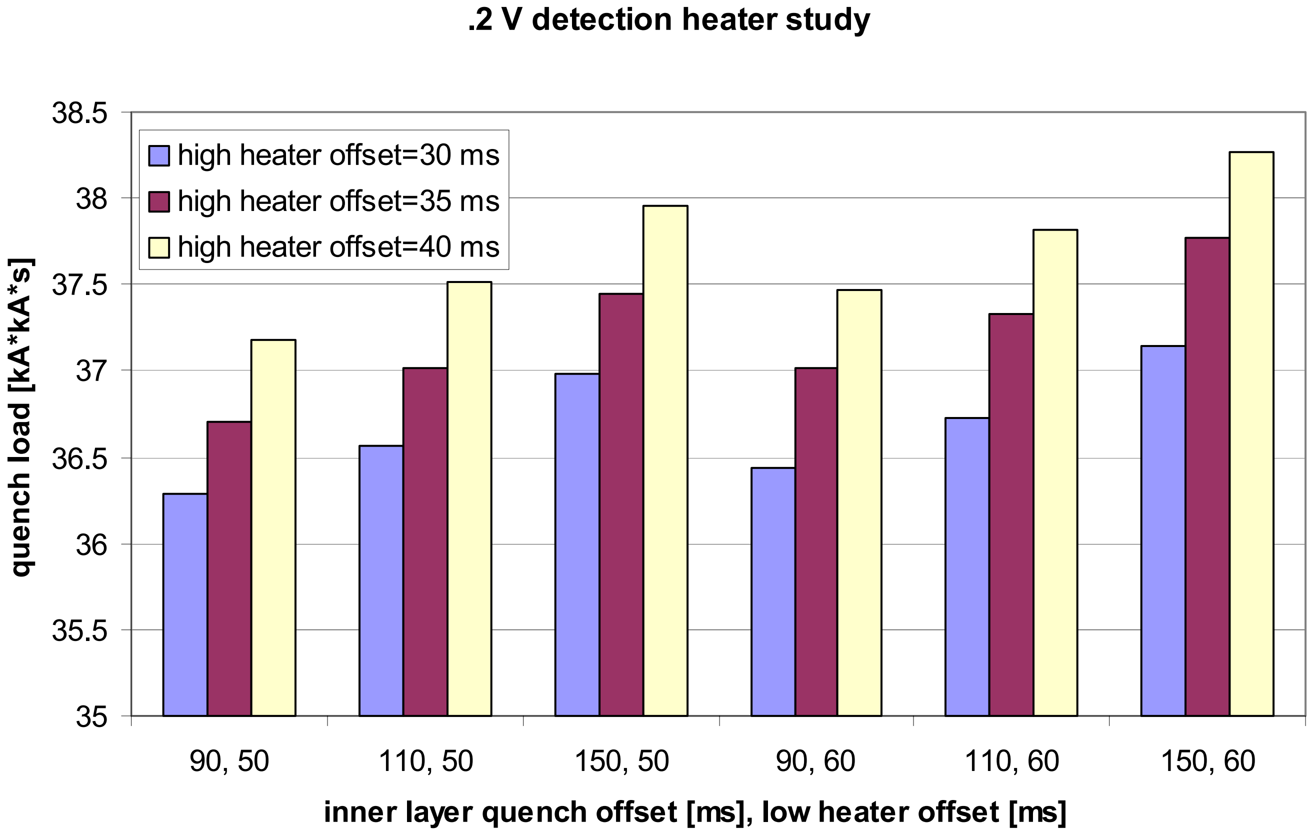

Figure 17

3.3. Aperture quenching asymmetries (scattering)

Four series of simulations were run to determine the effects of differences between aperture firing times. In all simulations, the quench originates in aperture 1. First high field heater asymmetries were examined. The firing time differences in Figure 18 indicate which aperture fired late and by what amount of time. Small firing differences have only small effects (quench time of inner layer held constant).

Similar simulations were carried out to study low field heater asymmetries. Here (see Figure 19), the results show situations in which a heater fires early by a certain amount of time or fails. Failure of a half of the LF heaters is not serious.

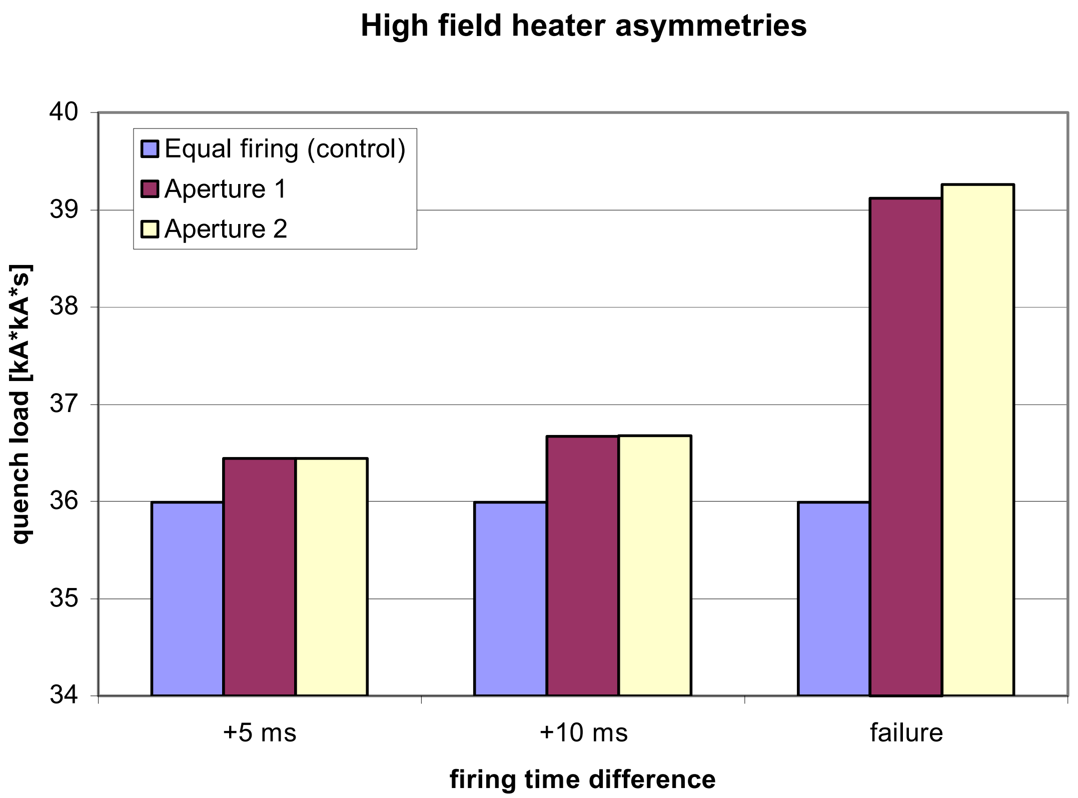

Figure 18

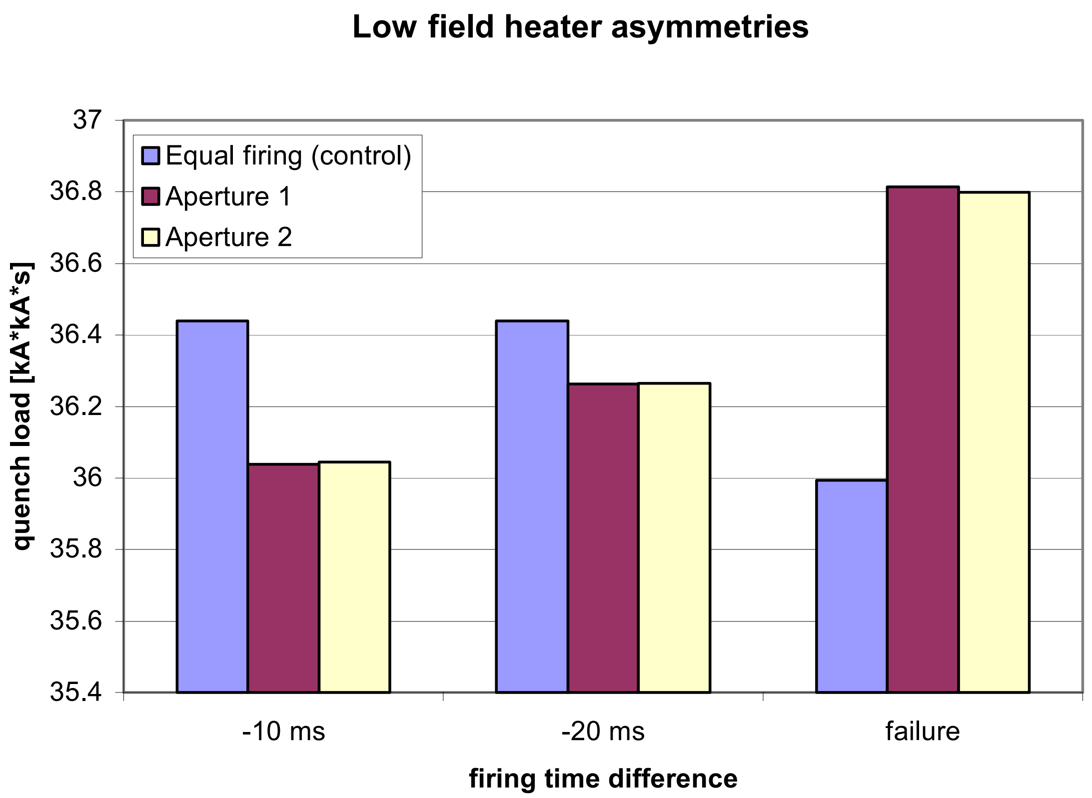

Figure 19

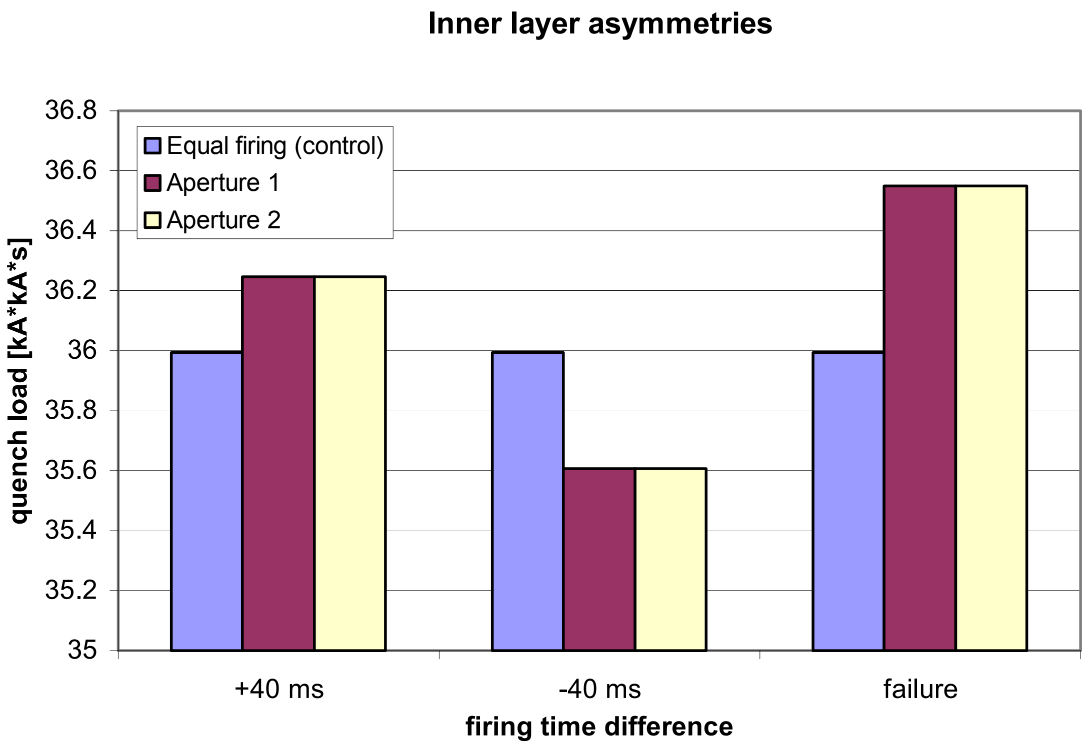

Figure 20

In the case of scattering of the inner layer quench time, it is apparent that this effect is very small compared to the effects of the heaters (see Figure 20), as the inner layer quenches much later.

The effects of an asymmetrical heater firing can be seen clearly in intra-magnet voltages. Figures 21 – 23 show effects of increasing scattering within the magnet. The most prominent effect is the increasing voltage in the part of the magnet containing the quench origin (outer layer, upper pole, aperture 1 as in Figure 1). Upper plots show aperture 2 voltages; aperture 1 voltages are below. The graphs were generated by SABER for each aperture, pole and layer in the magnet. For simplicity, all heat elements fire (and inner layer quench occurs) at the same time, viz. 110 ms, or late as indicated in the figures.

In Figures 22 and 23, note the increasing voltages in aperture 1. As the quench starts later in aperture 2, the inductive voltages dominate causing the voltages to decrease. Consequently the resistance development is taking place more in aperture 1, and, in the extreme case where no quench is allowed to propagate to aperture 2 (Figure 23), the outer layer voltages in aperture 1 rise to nearly 1000 V. In Figures 22 and 23, the voltages of the inner layers are predominately inductive and have negative voltages at some points because they do not have as much resistance development as the outer layers.

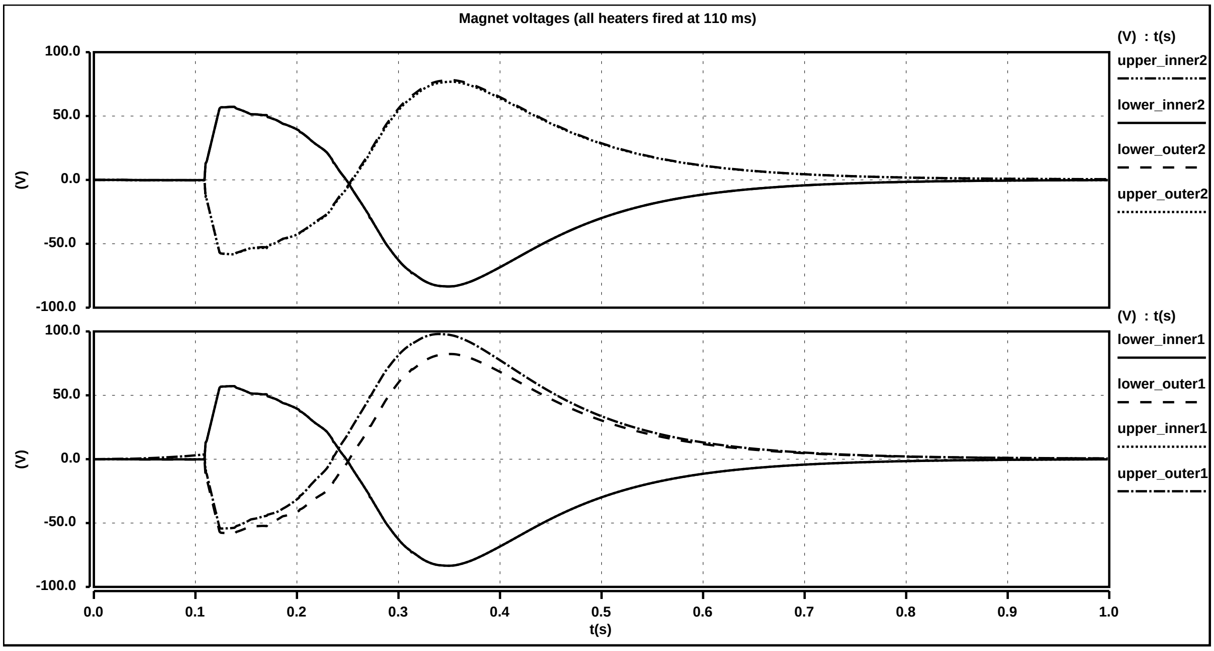

Figure 21: All heaters firing together (normal situation)

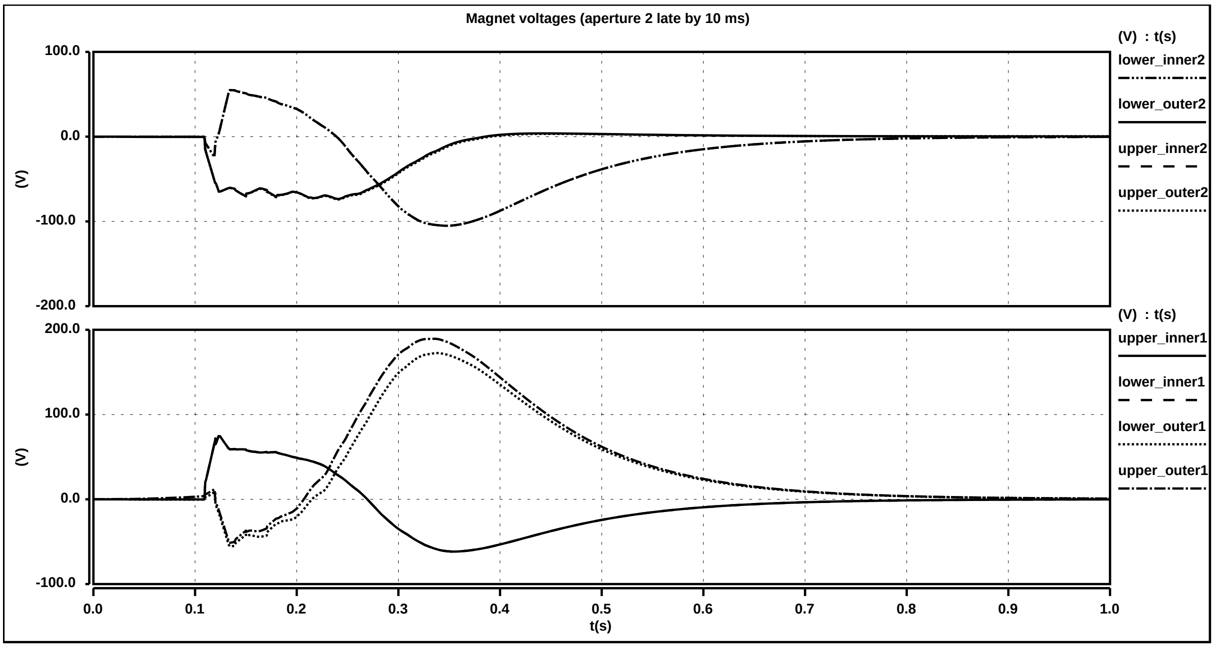

Figure 22: Aperture 2 quenches 10 ms late

The final asymmetry study assesses the situation where three components fail in a magnet. In Figure 24, A = aperture, LF = low field heater failure, HF = high field heater failure, and IN = no quench in inner layer. Thus, in A2 failure, for example, the aperture never quenches (since in QUABER the quenching of the aperture opposite the quench origin must be initiated by a "heat" element). These values were generated using 0.2 V detection with a 5 ms validation period.

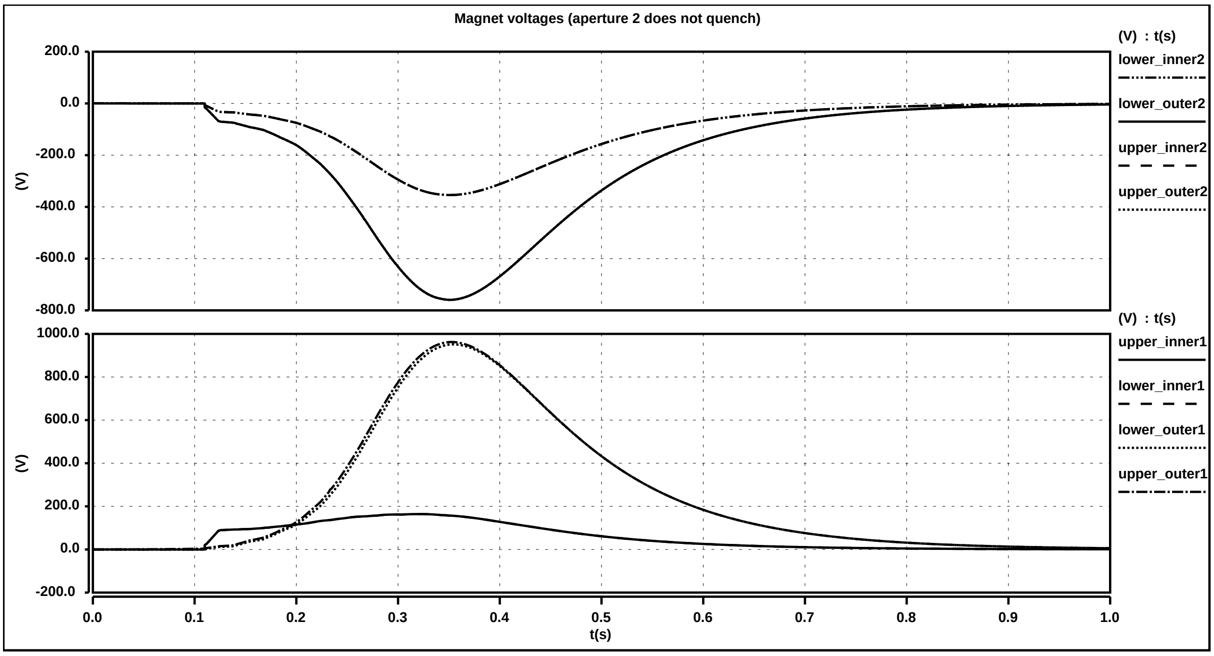

Figure 23: No quench in aperture 2 (no heaters fired, no inner layer quench)

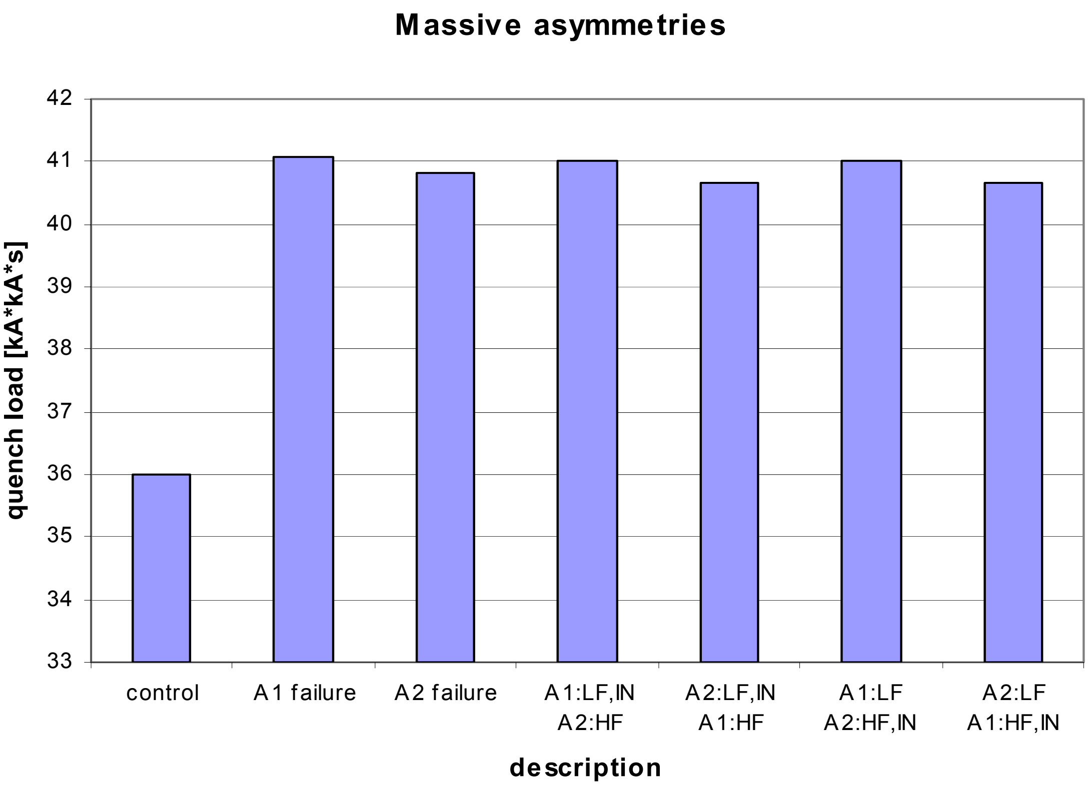

Figure 24

3.4. Remarks

A detection level of 0.2 V is acceptable, which corresponds to a 0.1 V detection threshold entering the detection circuitry from the bridge. In all cases, the protection diode turned on, even at an injection current level of 0.8 kA without heaters being effective. Heaters are not necessary for protection until approximately 2 kA. High field heaters are much more effective than low field heaters at protecting a quenching magnet. High field heaters alone should offer sufficient protection. Small differences between heater delays in different apertures do not cause dangerous intra-magnet voltages.

4. Acknowledgements

Thanks to R. Schmidt for his support and proofreading and to F. Rodriguez Mateos for many suggestions, as well as the rest of ICP for their help. Thanks to S. Russenschuck for providing the required design parameters. Thanks to all of MTA for their measurements that allow calibrating the simulation model.

5. References

1. F. Rodriguez et al., QUABER 4.0 User Guide.
2. F. Sonnemann et al., Quench process and protection of LHC dipole magnets, LHC Project Note 184
3. F. Rodriguez et al., The protection system for the superconducting elements of the LHC of CERN, LHC Project Report 283
4. R. Schmidt., Private communication.
5. A. Siemko., Private communication.

APPENDIX A: DATA FOR MAGNET CURRENT EFFECTS

CURRENT STUDY ON MB DIPOLE MAGNET

	for detection…no heaters firing				heater delay offsets…					
current [kA]	**t (.1V) [ms]**	**t(.2V) [ms]**	**t(.3V) [ms]**	**t(.5V) [ms]**	**high [ms]**	**low [ms]**	**quench velocity [m/s]**	**ttx [ms]**	**peakfield**	**filename**
0.8	824.5	1442.4	2060.2	3268.8	232.9	241.4	1.36	58.8	0.58	*mbcurrent001.sin*
1.5	332.1	497.8	656.5	967.98	204.6	218.9	2.54	50.2	1.09	*mbcurrent002.sin*
3	128.3	179.2	233.2	304.31	155.0	177.4	5.09	42.2	2.19	*mbcurrent003.sin*
4.5	77.6	109.9	124.2	167.14	117.4	143.8	7.63	38.2	3.28	*mbcurrent0045.sin*
6	57.6	73.2	80.9	111.16	89.0	116.6	10.17	35.5	4.38	*mbcurrent004.sin*
9	26.7	35.9	47.3	59.362	51.1	76.6	15.26	32.1	6.57	*mbcurrent005.sin*
11.796	19.1	26.1	31.1	41.396	30.5	51.8	20.00	30.0	8.61	*mbcurrent006.sin*
11.796 single	14.699	23.216	30	41.018						
11	just for the final hhh simulations						18.65	30.5	8.03	
11.796origmov	25.578	37.378	45.965	58.368						mborig.sin
11.796RRRlow	12.4	18.71	24.64	34.9						
RRRloworigmov	19.2	30.99	38.9	49.66						

using 5ms swdel offset from time of detection for validation, heater delays below calculated using the offsets above

<u>GROUP 1: detection at .1V</u>

						RESULTS				
current [kA]	**swdel [ms]**	**high heaters [ms]**	**low heaters [ms]**	**inner heaters [ms]**	**filename**	**miits [kA*kA*s]**	**hot spot [K]**	**resistive dev [Ohm]**	**max Vmag [V]**	**time of max V [s]**
0.8	829.5	1062.4	1070.9	do not fire	*mbcurrent101.sin*	2.2717	22.601	0.023	8.3	1.1967
1.5	337.1	541.7	556.0	do not fire	*mbcurrent102.sin*	6.046	32.871	0.029	8.3	0.6053
3	133.3	288.3	310.7	do not fire	*mbcurrent103.sin*	14.654	56.473	0.073	8.3	0.3114
6	62.6	151.5	179.1	299.1	*mbcurrent104.sin*	24.79	125.77	0.292	8.3	0.1567
9	31.7	82.7	108.2	188.2	*mbcurrent105.sin*	31.44	239.35	0.679	8.3	0.0856
11.796	24.1	54.6	75.9	125.9	*mbcurrent106.sin*	35.963	377.38	1.174	8.3	0.0567

<u>GROUP 2: detection at .2V</u>

current [kA]	**swdel [ms]**	**high heaters [ms]**	**low heaters [ms]**	**inner heaters [ms]**	**filename**					
0.8	1447.4	1680.3	1688.8	do not fire	*mbcurrent201.sin*	2.6559	23.634	0.023	8.3	1.8145
1.5	502.8	707.4	721.7	do not fire	*mbcurrent202.sin*	6.422	33.658	0.029	8.3	0.7707
3	184.2	339.2	361.6	do not fire	*mbcurrent203.sin*	15.117	57.787	0.07277	8.3	0.3624
6	78.2	167.2	194.8	314.8	*mbcurrent204.sin*	25.356	131.05	0.29181	8.3	0.1724
9	40.9	91.9	117.4	197.4	*mbcurrent205.sin*	32.175	252.87	0.71131	8.3	0.0947
11.796	31.1	61.5	82.9	132.9	*mbcurrent206.sin*	36.924	406.05	1.1726	8.3	0.0636

<u>GROUP 3: detection at .5V</u>

current [kA]	**swdel [ms]**	**high heaters [ms]**	**low heaters [ms]**	**inner heaters [ms]**	**filename**					
0.8	3273.8	3506.7	3515.2	do not fire	*mbcurrent501.sin*	3.767	26.54	0.02245	8.3	3.6405
1.5	973.0	1177.6	1191.8	do not fire	*mbcurrent502.sin*	7.469	35.827	0.02908	8.3	1.2399
3	309.3	464.3	486.7	do not fire	*mbcurrent503.sin*	16.192	61.659	0.07272	8.3	0.4874
6	116.2	205.1	232.7	352.7	*mbcurrent504.sin*	26.719	144.73	0.29164	8.3	0.21001
9	64.4	115.4	140.9	220.9	*mbcurrent505.sin*	34.064	291.31	0.71105	8.3	0.1181
11.796	46.4	76.8	98.2	148.2	*mbcurrent506.sin*	39.035	477.09	1.1716	8.3	0.07871

<u>FAILURE 1: heater failure at .8 kA (inner heaters not fired in any of these trials)</u>

						RESULTS				
detection V	**swdel [ms]**	**high heaters [ms]**	**low heaters [ms]**	**inner heaters [ms]**	**filename**	**miits [kA*kA*s]**	**hot spot [K]**	**resistive dev [Ohm]**	**max Vmag [V]**	**time of max V [s]**
0.1	829.5	1062.4	failure	do not fire	*mbfailure1a.sin*	3.0325	24.646	0.0145	8.3	1.3593
0.1	829.5	failure	1070.9		*mbfailure1b.sin*	3.0702	24.748	0.0156	8.3	1.473
0.1	829.5	failure	failure		*mbfailure1c.sin*	29.567	120.9	0.0382	8.3	100.8
0.2	1447.4	1680.3	failure		*mbfailure2a.sin*	3.5945	26.126	0.014557	8.3	1.9772
0.2	1447.4	failure	1688.8		*mbfailure2b.sin*	3.5956	26.041	0.015811	8.3	2.0665
0.2	1447.4	failure	failure		*mbfailure2c.sin*	29.117	117.11	0.03647	8.3	91.443
0.5	3273.8	3506.7	failure		*mbfailure5a.sin*	4.7163	28.77	0.01448	8.3	3.803
0.5	3273.8	failure	3515.2		*mbfailure5b.sin*	4.6675	28.701	0.01606	8.3	3.8859
0.5	3273.8	failure	failure		*mbfailure5c.sin*	28.485	112.12	0.0343	8.3	79.207
no detection	infinite	failure	failure		*mbfailure6a.sin*	26.427	97.402	0.028499	8.3	37.645

<u>FAILURE 2: heater failure at 1.5 kA (inner heaters not fired in any of these trials)</u>

						RESULTS				
detection V	**swdel [ms]**	**high heaters [ms]**	**low heaters [ms]**	**inner heaters [ms]**	**filename**	**miits [kA*kA*s]**	**hot spot [K]**	**resistive dev [Ohm]**	**max Vmag [V]**	**time of max V [s]**
0.1	337.1	failure	failure	do not fire	*mbfailure102.sin*	28.14	123.07	0.0379	8.3	10.708
0.2	502.8	failure	failure		*mbfailure202.sin*	28.94	123.29	0.038	8.3	10.619
0.5	973	failure	failure		*mbfailure502.sin*	28.973	123.58	0.0381	8.3	10.553
no detection	infinite	failure	failure		*mbfailure602.sin*	29.412	127.45	0.0401	8.3	9.148

<u>FAILURE 3: heater failure at 3 kA (inner heaters not fired in any of these trials)</u>

						RESULTS				
detection V	**swdel [ms]**	**high heaters [ms]**	**low heaters [ms]**	**inner heaters [ms]**	**filename**	**miits [kA*kA*s]**	**hot spot [K]**	**resistive dev [Ohm]**	**max Vmag [V]**	**time of max V [s]**
0.1	133.3	failure	failure	do not fire	*mbfailure103.sin*	38.818	289.92	0.2054	8.3	2.799
0.2	184.2	failure	failure		*mbfailure203.sin*	38.827	290.11	0.2056	8.3	2.8
0.5	309.3	failure	failure		*mbfailure503.sin*	38.848	290.57	0.206	8.3	2.794
no detection	infinite	failure	failure		*mbfailure603.sin*	39.183	297.97	0.1322	8.3	2.5318

<u>FAILURE 4: heater failure at 4.5 kA (inner heaters not fired in any of these trials)</u>

						RESULTS				
detection V	**swdel [ms]**	**high heaters [ms]**	**low heaters [ms]**	**inner heaters [ms]**	**filename**	**miits [kA*kA*s]**	**hot spot [K]**	**resistive dev [Ohm]**	**max Vmag [V]**	**time of max V [s]**
0.1	82.6	failure	failure	do not fire	*mbfailure45a.sin*	48.229	663.11	0.42752	8.3	1.5689
0.2	114.9	failure	failure		*mbfailure45b.sin*	48.236	663.46	0.42769	8.3	1.5685
0.5	129.2	failure	failure		*mbfailure45c.sin*	48.239	663.61	0.42433	8.3	1.5682
no detection	infinite	failure	failure		*mbfailure45d.sin*	48.874	696.73	0.34386	8.3	1.4291

<u>FAILURE 5: heater failure at 6 kA (inner heaters not fired in any of these trials)</u>

						RESULTS				
detection V	**swdel [ms]**	**high heaters [ms]**	**low heaters [ms]**	**inner heaters [ms]**	**filename**	**miits [kA*kA*s]**	**hot spot [K]**	**resistive dev [Ohm]**	**max Vmag [V]**	**time of max V [s]**
0.1	62.6	failure	failure	do not fire	*mbfailure104.sin*	52.8	1037.8	0.51306	8.3	1.1614
0.2	78.2	failure	failure		*mbfailure204.sin*	52.803	1038	0.51306	8.3	1.1613
0.5	116.2	failure	failure		*mbfailure504.sin*	52.81	1038.6	0.51364	8.3	1.1607
no detection	infinite	failure	failure		*mbfailure604.sin*	54.205	1146.3	0.53928	8.3	1.0436

APPENDIX B: HEATER STUDY DATA

PARAMETER STUDY AT 11796 A (quench velocity = 1500 cm/sec)

Template	Detection [V]	Validation [ms]	swdel [ms]	High heaters [ms]	Low heaters [ms]	Inner heaters [ms]	Hot spot [K]	Vmax [V]	t of Vmag [s]	resdev [Ohm]	miits [kA*kA*s]	idot @tinner [A/s]	filename
Series	0.1	5	24.1	54.1	74.1	134.1	366.99	8.3	0.056192	1.1308	35.562	-6885.7	*mb1.sin*
Series	0.1	5	24.1	54.1	74.1	174.1	378.93	8.3	0.056192	1.1444	36.016	-16873	*mb2.sin*
Series	0.1	5	24.1	54.1	84.1	144.1	375.35	8.3	0.056192	1.1353	35.891	-8284.2	*mb3.sin*
Series	0.1	5	24.1	54.1	84.1	184.1	385.06	8.3	0.056192	1.145	36.227	-18265	*mb4.sin*
Series	0.1	5	24.1	59.1	79.1	139.1	386.83	8.3	0.061171	1.1308	36.288	-6888.4	*mb5.sin*
Series	0.1	5	24.1	59.1	79.1	179.1	399.43	8.3	0.061171	1.1453	36.709	-16872	*mb6.sin*
Series	0.1	5	24.1	59.1	89.1	149.1	395.66	8.3	0.061171	1.1348	36.584	-8232.6	*mb7.sin*
Series	0.1	5	24.1	59.1	89.1	189.1	405.92	8.3	0.061171	1.1445	36.92	-18364	*mb8.sin*
Series	0.1	10	29.1	59.1	79.1	139.1	386.86	8.3	0.061176	1.1309	36.289	-6889.2	*mb9.sin*
Series	0.1	10	29.1	59.1	79.1	179.1	399.47	8.3	0.061176	1.1454	36.71	-16875	*mb10.sin*
Series	0.1	10	29.1	59.1	89.1	149.1	395.7	8.3	0.061176	1.1349	36.585	-8223.8	*mb11.sin*
Series	0.1	10	29.1	59.1	89.1	189.1	405.95	8.3	0.061176	1.1446	36.921	-18367	*mb12.sin*
Series	0.1	10	29.1	64.1	84.1	144.1	407.78	8.3	0.066139	1.1302	36.981	-6944.6	*mb13.sin*
Series	0.1	10	29.1	64.1	84.1	184.1	421.09	8.3	0.066139	1.1447	37.402	-16883	*mb14.sin*
Series	0.1	10	29.1	64.1	94.1	154.1	417.11	8.3	0.066139	1.1342	37.277	-8237.4	*mb15.sin*
Series	0.1	10	29.1	64.1	94.1	194.1	427.93	8.3	0.066139	1.1439	37.613	-18286	*mb16.sin*
Series	0.2	5	31.1	61.1	81.1	141.1	395.12	8.3	0.063164	1.1307	36.566	-6890.6	*mb17.sin*
Series	0.2	5	31.1	61.1	81.1	181.1	407.9	8.3	0.063164	1.1448	36.985	-16891	*mb18.sin*
Series	0.2	5	31.1	61.1	91.1	151.1	404.15	8.3	0.063164	1.1346	36.863	-8300	*mb19.sin*
Series	0.2	5	31.1	61.1	91.1	191.1	414.63	8.3	0.063164	1.1443	37.198	-18282	*mb20.sin*
Series	0.2	5	31.1	66.1	86.1	146.1	416.49	8.3	0.068129	1.1299	37.258	-6901.1	*mb21.sin*
Series	0.2	5	31.1	66.1	86.1	186.1	430.08	8.3	0.068129	1.1444	37.678	-16888	*mb22.sin*
Series	0.2	5	31.1	66.1	96.1	156.1	426.03	8.3	0.068129	1.1339	37.554	-8239.5	*mb23.sin*
Series	0.2	5	31.1	66.1	96.1	196.1	437.09	8.3	0.068129	1.1436	37.89	-184055	*mb24.sin*
Series	0.2	5	31.1	61.1	81.1	121.1	386.75	8.3	0.063164	1.1268	36.285	-5196.7	*mb50.sin*
Series	0.2	5	31.1	61.1	91.1	121.1	391.31	8.3	0.063164	1.1264	36.439	-4761.4	*mb51.sin*
Series	0.2	5	31.1	61.1	91.1	141.1	399.83	8.3	0.063164	1.1294	36.722	-6926.5	*mb52.sin*
Series	0.2	5	31.1	61.1	91.1	181.1	412.75	8.3	0.036164	1.1416	37.139	-14886	*mb53.sin*
Series	0.2	5	31.1	66.1	81.1	121.1	399.35	8.3	0.068129	1.1262	36.706	-4985.5	*mb54.sin*
Series	0.2	5	31.1	66.1	81.1	141.1	408.77	8.3	0.068129	1.1304	37.013	-6431.2	*mb55.sin*
Series	0.2	5	31.1	66.1	81.1	181.1	422.4	8.3	0.068129	1.1444	37.442	-15692	*mb56.sin*
Series	0.2	5	31.1	66.1	91.1	121.1	408.97	8.3	0.068129	1.1175	37.019	-4449.9	*mb57.sin*
Series	0.2	5	31.1	66.1	91.1	141.1	418.87	8.3	0.068129	1.1261	37.332	-6395.4	*mb58.sin*
Series	0.2	5	31.1	66.1	91.1	181.1	433.17	8.3	0.068129	1.1342	37.772	-13569	*mb59.sin*
Series	0.2	5	31.1	71.1	81.1	121.1	413.86	8.3	0.073108	1.1298	37.174	-4658.7	*mb60.sin*
Series	0.2	5	31.1	71.1	81.1	141.1	424.71	8.3	0.073108	1.1353	37.513	-6448.4	*mb61.sin*
Series	0.2	5	31.1	71.1	81.1	181.1	439.3	8.3	0.073108	1.1487	37.956	-14458	*mb62.sin*
Series	0.2	5	31.1	71.1	91.1	121.1	423.16	8.3	0.073108	1.1217	37.466	-4120.4	*mb63.sin*
Series	0.2	5	31.1	71.1	91.1	141.1	434.77	8.3	0.073108	1.1287	37.82	-6205.7	*mb64.sin*
Series	0.2	5	31.1	71.1	91.1	181.1	450.12	8.3	0.073108	1.1376	38.274	-12514	*mb65.sin*
Series	0.2	10	36.1	66.1	86.1	146.1	416.53	8.3	0.068131	1.13	37.259	-6902	*mb33.sin*
Series	0.5	5	46.4	76.4	96.4	156.4	463.79	8.3	0.078386	1.127	38.665	-6998.3	*mb25.sin*
Series	0.5	5	46.4	76.4	96.4	196.4	478.95	8.3	0.078386	1.1418	39.086	-17008	*mb26.sin*
Series	0.5	5	46.4	76.4	106.4	166.4	474.45	8.3	0.078386	1.1312	38.962	-8305.7	*mb27.sin*
Series	0.5	5	46.4	76.4	106.4	206.4	486.78	8.3	0.078386	1.1408	39.297	-18415	*mb28.sin*
Series	0.5	5	46.4	81.4	101.4	161.4	489.58	8.3	0.083362	1.1273	39.373	-6912.9	*mb29.sin*
Series	0.5	5	46.4	81.4	101.4	201.4	505.5	8.3	0.083362	1.1416	39.79	-16949	*mb30.sin*
Series	0.5	5	46.4	81.4	111.4	171.4	500.78	8.3	0.083362	1.1311	39.668	-8317.2	*mb31.sin*
Series	0.5	5	46.4	81.4	111.4	211.4	513.9	8.3	0.083362	1.1411	40.005	-18344	*mb32.sin*
Series	0.5	10	51.4	81.4	101.4	161.4	489.62	8.3	0.083364	1.1274	39.374	-6913.7	*mb34.sin*
Single	0.1	5	24.1	54.1	74.1	134.1	347.45	-235.67	0.0241	1.0407	34.873	-9017.2	*mb1s.sin*
Single	0.1	5	24.1	59.1	89.1	189.1	386.62	-235.67	0.0241	1.0479	36.281	-20345	*mb8s.sin*
Single	0.1	10	29.1	59.1	79.1	139.1	366.05	-235.67	0.0291	1.0396	35.561	-8833.3	*mb9s.sin*
Single	0.1	10	29.1	64.1	94.1	194.1	407.59	-235.67	0.0291	1.047	36.975	-20354	*mb16s.sin*
Single	0.2	5	31.1	61.1	81.1	141.1	373.46	-236.14	0.0311	1.0405	35.824	-8834.2	*mb17s.sin*
Single	0.2	5	31.1	66.1	96.1	196.1	416.28	-236.14	0.0311	1.0468	37.251	-20359	*mb24s.sin*
Single	0.5	5	46.4	76.4	96.4	156.4	439.1	-235.67	0.0464	1.0369	37.95	-8914.7	*mb25s.sin*
Single	0.5	5	46.4	81.4	111.4	211.4	489.3	-235.67	0.0464	1.0436	39.365	-20403	*mb32s.sin*

APPENDIX C: DATA FOR APERTURE QUENCH ASYMMETRIES

Heater delay aperture tests. Detection at .2V with 5 ms validation period

		APERTURE 1 [ms]			APERTURE 2 [ms]				Maximum intramagnet voltages occuring (not necessarily at the same time)							
filename	swdel	high field	low field	inner	high field	low field	inner	MIITS	upper_outer1	upper_inner1	lower_inner1	lower_outer1	upper_outer2	upper_inner2	lower_inner2	lower_outer2
mbh1.sin	31.1	**61.1**	81.1	121.1	**66.1**	81.1	121.1	36.439	287.3	-265.41	-265.41	305.39	234.05	-265.41	-265.41	235.59
mbh2.sin	31.1	**66.1**	81.1	121.1	**61.1**	81.1	121.1	36.439	221.48	-265.42	-265.42	239.24	300.05	-265.42	-265.42	301.58
mbh3.sin	31.1	**61.1**	81.1	121.1	**61.1**	81.1	121.1	35.993	246.96	-257.02	-257.02	263.54	258.38	-257.02	-257.02	259.9
mbh4.sin	31.1	**61.1**	81.1	121.1	**71.1**	81.1	121.1	36.674	329.49	-255.09	-255.09	348.29	170.81	-255.09	-255.09	172.43
mbh5.sin	31.1	**71.1**	81.1	121.1	**61.1**	81.1	121.1	36.671	167.72	-257.67	-257.67	176.59	342.73	-257.67	-257.67	344.29
mbh3.sin	31.1	**61.1**	81.1	121.1	**61.1**	81.1	121.1	35.993	246.96	-257.02	-257.02	263.54	258.38	-257.02	-257.02	259.9
mbh20.sin	31.1	**61.1**	81.1	121.1	**failure**	81.1	121.1	39.26	764.65	-166	-166	795.41	-452.99	-166	-166	-452.99
mbh21.sin	31.1	**failure**	81.1	121.1	**61.1**	81.1	121.1	39.12	-377.33	-173.06	-173.06	-497.02	782.64	-173.06	-173.06	784.49
mbh3.sin	31.1	**61.1**	81.1	121.1	**61.1**	81.1	121.1	35.993	246.96	-257.02	-257.02	263.54	258.38	-257.02	-257.02	259.9
mbh6.sin	31.1	61.1	**71.1**	121.1	61.1	**91.1**	121.1	36.039	301.06	-265.15	-265.15	321.34	218.76	-265.15	-265.15	220.22
mbh7.sin	31.1	61.1	**91.1**	121.1	61.1	**71.1**	121.1	36.045	202.58	-265	-265	224.3	316.21	-265	-265	317.67
mbh8.sin	31.1	61.1	**91.1**	121.1	61.1	**91.1**	121.1	36.439	249.79	-265.23	-265.23	273.29	268.55	-265.23	-265.23	270.04
mbh9.sin	31.1	61.1	**81.1**	121.1	61.1	**91.1**	121.1	36.262	273.13	-266.03	-266.03	294.94	247.59	-266.03	-266.03	249.17
mbh10.sin	31.1	61.1	**91.1**	121.1	61.1	**81.1**	121.1	36.264	230.25	-265.98	-265.98	252.57	290.1	-265.98	-265.98	291.69
mbh8.sin	31.1	61.1	**91.1**	121.1	61.1	**91.1**	121.1	36.439	249.79	-265.23	-265.23	273.29	268.55	-265.23	-265.23	270.04
mbh22.sin	31.1	61.1	**81.1**	121.1	61.1	**failure**	121.1	36.799	353.88	-247.88	-247.88	372.67	132.04	-247.88	-247.88	133.61
mbh23.sin	31.1	61.1	**failure**	121.1	61.1	**81.1**	121.1	36.815	114.13	-247.35	-247.35	134.35	369.99	-247.35	-247.35	371.57
mbh3.sin	31.1	61.1	**81.1**	121.1	61.1	**81.1**	121.1	35.993	246.96	-257.02	-257.02	263.54	258.38	-257.02	-257.02	259.9
mbh11.sin	31.1	61.1	81.1	**121.1**	61.1	81.1	**161.1**	36.246	279.92	-256.94	-256.94	297.24	291.9	-323.97	-323.97	293.43
mbh12.sin	31.1	61.1	81.1	**161.1**	61.1	81.1	**121.1**	36.246	279.92	-323.97	-323.97	297.24	291.9	-256.94	-256.94	293.43
mbh3.sin	31.1	61.1	81.1	**121.1**	61.1	81.1	**121.1**	35.993	246.96	-257.02	-257.02	263.54	258.38	-257.02	-257.02	259.9
mbh13.sin	31.1	61.1	81.1	**121.1**	61.1	81.1	**91.1**	35.607	206.08	-261.88	-261.88	225.53	220.73	-175.02	-175.02	222.2
mbh14.sin	31.1	61.1	81.1	**91.1**	61.1	81.1	**121.1**	35.606	206.15	-175.1	-175.1	225.63	220.79	-261.95	-261.95	222.26
mbh3.sin	31.1	61.1	81.1	**121.1**	61.1	81.1	**121.1**	35.993	246.96	-257.02	-257.02	263.54	258.38	-257.02	-257.02	259.9
mbh24.sin	31.1	61.1	81.1	**121.1**	61.1	81.1	**failure**	36.549	325.98	-253.71	-253.71	344.17	338.61	-420.45	-420.45	340.19
mbh25.sin	31.1	61.1	81.1	**failure**	61.1	81.1	**121.1**	36.549	325.98	-420.45	-420.45	344.17	338.61	-253.71	-253.71	340.19
mbh3.sin	31.1	61.1	81.1	**121.1**	61.1	81.1	**121.1**	35.993	246.96	-257.02	-257.02	263.54	258.38	-257.02	-257.02	259.9
mbh26.sin	31.1	61.1	81.1	121.1	failure	failure	failure	41.086	1216.7	-102.67	-102.67	1256	-773.05	-360.59	-360.59	-773.05
mbh27.sin	31.1	failure	failure	failure	61.1	81.1	121.1	40.813	-632.51	-364.16	-364.16	-780.7	1182.7	-113.2	-113.2	1184.1
mbh3.sin	31.1	61.1	81.1	121.1	61.1	81.1	121.1	35.993	246.96	-257.02	-257.02	263.54	258.38	-257.02	-257.02	259.9
mbh28.sin	31.1	61.1	failure	failure	failure	81.1	121.1	41.012	765.93	-360.34	-360.34	806.85	-332.7	-104.65	-104.65	-332.7
mbh29.sin	31.1	failure	81.1	121.1	61.1	failure	failure	40.67	-219.28	-118.07	-118.07	-349.07	747.45	-365.06	-365.06	748.94
mbh3.sin	31.1	61.1	81.1	121.1	61.1	81.1	121.1	35.993	246.96	-257.02	-257.02	263.54	258.38	-257.02	-257.02	259.9
mbh30.sin	31.1	61.1	failure	121.1	failure	81.1	failure	41.013	765.93	-104.65	-104.65	806.85	-332.7	-360.34	-360.34	-332.7
mbh31.sin	31.1	failure	81.1	failure	61.1	failure	81.1	40.67	-219.3	-365.1	-365.1	-349.1	747.53	-118.07	-118.07	749.02
mbh3.sin	31.1	61.1	81.1	**121.1**	61.1	81.1	**121.1**	35.993	246.96	-257.02	-257.02	263.54	258.38	-257.02	-257.02	259.9